

PREPARED FOR SUBMISSION TO JHEP

# Next-to-leading order contributions to the pole mass of gluino in minimal gauge mediation

---

Jae Yong Lee,<sup>a</sup> and Yeo Woong Yoon<sup>b</sup>

<sup>a</sup>*Department of Physics, Korea University,  
Seoul 136-701, Korea*

<sup>b</sup>*School of Physics, KIAS,  
Seoul 130-722, Korea*

*E-mail:* [littlehiggs@korea.ac.kr](mailto:littlehiggs@korea.ac.kr), [ywoon@kias.re.kr](mailto:ywoon@kias.re.kr)

**ABSTRACT:** We compute the pole mass of the gluino in the minimal gauge mediation to two-loop order. The pole mass of the gluino begins to arise at one-loop order and the two-loop order correction shifts the leading order pole mass by 20% or even more. This shift is much larger than the expected accuracy of the mass determination at the LHC, and should be reckoned with for precision studies on the SUSY breaking parameters.

**KEYWORDS:** gauge mediation, renormalization, supersymmetry breaking, NLO

**ARXIV EPRINT:** [1112.3904](https://arxiv.org/abs/1112.3904)

---

## Contents

<b>1</b>	<b>Introduction</b>	<b>1</b>
<b>2</b>	<b>Self-energy functions and pole masses for two-component spinors</b>	<b>2</b>
<b>3</b>	<b>Minimal gauge mediation</b>	<b>4</b>
3.1	Lagrangian of minimal gauge mediation	4
3.2	Feynman rules	5
<b>4</b>	<b>Renormalization</b>	<b>7</b>
<b>5</b>	<b>Self-energy functions</b>	<b>10</b>
5.1	Self-energy functions at one-loop order	10
5.2	Self-energy function at two-loop order	13
<b>6</b>	<b>Numerical Analysis</b>	<b>16</b>
<b>7</b>	<b>Conclusion and Outlook</b>	<b>19</b>
<b>A</b>	<b>Master Integrals</b>	<b>20</b>
<b>B</b>	<b>Explicit formula for <math>\Omega^{(2)}(s)</math></b>	<b>30</b>

---

## 1 Introduction

Supersymmetry, an elegant extension of spacetime symmetry, is the leading candidate for the new physics unfolded in the Large Hadron Collider (LHC) at CERN. The two detectors ATLAS and CMS of the LHC have been collecting data at a much faster than expected and their recent data significantly extend the exclusion limits for supersymmetric particles. But the latest such data have so far been interpreted by the experiment in only two different supersymmetry breaking models: the constrained minimal supersymmetric standard model (CMSSM) and a simplified model with only squarks and gluinos and massless neutralinos.

Other supersymmetry breaking models should be extensively analyzed in the era of the LHC. One of those to be analyzed is gauge mediated supersymmetry breaking (GMSB) model [1–9] where messenger fields, charged under the Standard Model gauge symmetry, mediate the breakdown of supersymmetry in the hidden sector to the MSSM sector. The soft masses in the visible sector arise from quantum effects of the messengers so the supersymmetry breaking scale of the visible sector is much lowered than the grand unified theory (GUT) scale compared with the gravity mediated supersymmetry breaking scenario.

As the LHC continues to collect experimental data, the precise studies on the physical parameters of the SUSY particles will become important. This requires one to do quantum loop calculations on the SUSY parameters. For instance, the gluino pole mass of the CMSSM has been considered up to two-loop order in ref. [10–12] while the neutralino and chargino pole masses in ref. [13, 14].

Our interests lie in the gluino pole mass of the GMSB model at two-loop order. Among the various different GMSB models we choose the Minimal Gauge Mediation (MGM) where a pair of messenger fields, fundamental and antifundamental under the  $SU(3)_C$  gauge symmetry, mediate the supersymmetry breaking to the MSSM sector. The gluino pole mass of the GMSB model at two-loop order was first discussed in ref. [15] where the authors made a prediction that the NLO correction to the gluino pole mass is up to 10% of the LO pole mass. On the other hand, our prediction is, as shown later, 20% or even more. The difference between their and our predictions arises from how to handle the IR behavior of SUSY QCD. We state that our treatment of the IR behavior is more consistent with perturbative theory rather than theirs. We will rigorously discuss it in Section 5.

For the renormalization of the MGM lagrangian parameters the  $\overline{\text{DR}}$  scheme is adopted [16–18]. It is based on regularization by dimensional reduction along with modified minimal subtraction ( $\overline{\text{MS}}$ ) scheme. Not only the messenger fields wavefunctions but also their masses are renormalized. The MSSM quarks and squarks contribute to the gluino pole mass at two-loop order through the renormalization of the gluon(gluino) wavefunctions and the gauge coupling at one-loop order. We will also take these contributions into account.

In this paper, we follow the two-component formalism to derive the self-energy functions in ref. [12, 19], and then present the analytic results of the self-energy functions up to two-loop order relevant to the gluino pole mass. We also perform a numerical analysis for the NLO correction of the gluino pole mass.

## 2 Self-energy functions and pole masses for two-component spinors

We briefly review the self-energy functions for fermions in two-component notation and then describe how to compute the loop-corrected gluino pole mass of the MGM. All the details can be found in ref. [19].

We consider a theory with left-handed fermion degrees of freedom  $\psi_j$  with an index  $j = 1, 2, \dots, N$ . The self-energy functions for fermions in two-component notation are depicted in figure 1, where the shaded circles denote the sum of all one-particle irreducible(1PI), connected Feynman diagrams, and the external legs are amputated<sup>1</sup>. In figure 1 the self-energy functions for two-component fermions are denoted by  $\Xi, \Xi^T, \Omega$ , and  $\overline{\Omega}$ , and the four-momentum  $p$  flows from right to left.

The pole mass is defined by the position of the complex pole in the propagator and is a gauge-invariant and renormalization scale-invariant quantity. The pole mass of a fermion can be found by considering its rest frame, in which the space components of the external momentum  $p^\mu$  vanish. This reduces the spinor index dependence to a triviality. Setting

---

<sup>1</sup>At this stage, counterterm corrections are not reckoned with.

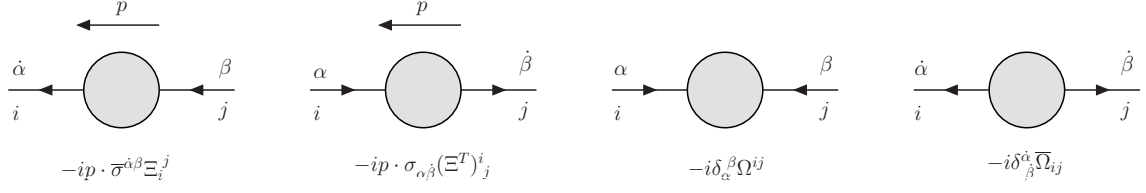


**Figure 1.** The self-energy functions for two-component fermions.

$p^\mu = (\sqrt{s}, 0)$ , we search for the values of  $s$ . In other words, the poles of the full propagator (which are in general complex)

$$s_{pole,j} \equiv (\mathbf{M}_j - i\mathbf{\Gamma}_j/2)^2 \quad (2.1)$$

are formally the solutions to the non-linear equation <sup>2</sup>

$$\det[s\mathbf{1} - (\mathbf{1} - \mathbf{\Xi}^T)^{-1}(\mathbf{m} + \mathbf{\Omega})(\mathbf{1} - \mathbf{\Xi})^{-1}(\bar{\mathbf{m}} + \bar{\mathbf{\Omega}})] = 0, \quad (2.2)$$

where  $\mathbf{m}_{ij}$  is the symmetric  $N \times N$  tree-level fermion mass matrix with  $\mathbf{m}_{ik}\bar{\mathbf{m}}^{kj} = m_i^2\delta_i^j$ .

The gluino pole mass of the MGM is zero at tree-level and arises at one-loop order. Moreover the gluino do not mix other fermions so the master equation reduces to a simple equation as

$$s - \frac{\Omega^2}{(1 - \Xi)^2} = 0. \quad (2.3)$$

The solution for Eq. (2.3) is given as

$$\sqrt{s} = \frac{\Omega}{1 - \Xi}, \quad (2.4)$$

and is perturbatively calculated as

$$\sqrt{s} = \Omega^{(1)} + [\Omega^{(1)}\Xi^{(1)} + \Omega^{(2)}] + \dots, \quad (2.5)$$

where the self-energy functions are expanded in powers of  $\alpha_s$ :

$$\Omega = \Omega^{(1)} + \Omega^{(2)} + \dots, \quad (2.6)$$

$$\Xi = \Xi^{(1)} + \Xi^{(2)} + \dots. \quad (2.7)$$

We use an iteration method to solve Eq. (2.5). We first get the leading order (LO) pole mass by substituting the tree level gluino mass ( $s = 0$ ) to the one-loop function  $\Omega(s)^{(1)}$ . Then we substitute the LO pole mass into Eq. (2.5) to calculate the NLO pole mass. In order to evaluate the gluino pole mass up to two-loop order we need to evaluate the self-energy functions  $\Omega^{(1)}$ ,  $\Omega^{(2)}$  and  $\Xi^{(1)}$ .

---

<sup>2</sup>Here  $\mathbf{M}_j$  and  $\mathbf{\Gamma}_j$  are a physical mass and width of a fermion.

### 3 Minimal gauge mediation

#### 3.1 Lagrangian of minimal gauge mediation

The chiral superfields contained in the MGM are messengers  $\Phi$  and  $\tilde{\Phi}$ , and a Goldstino multiplet  $X$ . The chiral superfield components corresponding to the chiral messenger field  $\Phi$  and  $\tilde{\Phi}$ , in the fundamental and anti-fundamental representation of the  $SU(3)_c$  gauge symmetry, are denoted as

$$\Phi = (\phi, \psi, \mathcal{F}), \quad \tilde{\Phi} = (\tilde{\phi}, \tilde{\psi}, \tilde{\mathcal{F}}). \quad (3.1)$$

The free lagrangian of the messenger fields and the SUSY Yang-Mills lagrangian are given as follows:

$$\begin{aligned} \mathcal{L}_{\text{free}} = & -\frac{1}{4}v_{\mu\nu}^a v^{a\mu\nu} + i\lambda^{\dagger a} \bar{\sigma}^\mu D_\mu \lambda^a + \frac{1}{2}\mathcal{D}^a \mathcal{D}^a \\ & + (D_\mu \phi)^\dagger (D^\mu \phi) + i\psi^\dagger \bar{\sigma}^\mu (D_\mu \psi) + \mathcal{F}^\dagger \mathcal{F} + (D_\mu \tilde{\phi})(D^\mu \tilde{\phi})^\dagger + i\tilde{\psi} \sigma^\mu (D_\mu \tilde{\psi}^\dagger) + \tilde{\mathcal{F}} \tilde{\mathcal{F}}^\dagger \\ & - \sqrt{2}g(\phi^\dagger \mathbf{T}^a \psi - \tilde{\psi} \mathbf{T}^a \tilde{\phi}^\dagger) \lambda^a - \sqrt{2}g\lambda^{a\dagger} (\psi^\dagger \mathbf{T}^a \phi - \tilde{\phi} \mathbf{T}^a \tilde{\psi}^\dagger) \\ & + g\mathcal{D}^a (\phi^\dagger \mathbf{T}^a \phi - \tilde{\phi} \mathbf{T}^a \tilde{\phi}^\dagger), \end{aligned} \quad (3.2)$$

where (i)  $g$  is the gauge coupling, (ii)  $f^{abc}$  are the antisymmetric structure constants of the gauge symmetry which satisfy

$$[\mathbf{T}^a, \mathbf{T}^b] = if^{abc} \mathbf{T}^c, \quad (3.3)$$

for the generators  $\mathbf{T}^a$  for the fundamental representation, (iii)  $\lambda^a$  is the gluino field, (iv)  $v_{\mu\nu}^a$  the gluon field strength,

$$v_{\mu\nu}^a = \partial_\mu v_\nu^a - \partial_\nu v_\mu^a - gf^{abc} v_\mu^b v_\nu^c, \quad (3.4)$$

(v)  $\mathcal{D}^a$  is the real auxiliary boson field, and (vi) the covariant derivatives are defined as

$$\begin{aligned} (D_\mu \phi)_i &= \partial_\mu \phi_i + igv_\mu^a (\mathbf{T}^a)_i^j \phi_j, \\ (D_\mu \tilde{\phi})^i &= \partial_\mu \tilde{\phi}^i - igv_\mu^a \tilde{\phi}^j (\mathbf{T}^a)_j^i, \\ (D_\mu \tilde{\phi})_i^\dagger &= \partial_\mu \tilde{\phi}_i^\dagger + igv_\mu^a (\mathbf{T}^a)_i^j \tilde{\phi}_j^\dagger, \\ (D_\mu \psi)_i &= \partial_\mu \psi_i + igv_\mu^a (\mathbf{T}^a)_i^j \psi_j, \\ (D_\mu \tilde{\psi}^\dagger)_i &= \partial_\mu \tilde{\psi}_i^\dagger + igv_\mu^a (\mathbf{T}^a)_i^j \tilde{\psi}_j^\dagger, \\ D_\mu \lambda^a &= \partial_\mu \lambda^a - gf^{abc} v_\mu^b \lambda^c. \end{aligned} \quad (3.5)$$

The Goldstino  $X$  couples to the messengers via a superpotential

$$W = X \tilde{\Phi} \Phi, \quad (3.6)$$

and has an expectation value:

$$\langle X \rangle = M + \theta^2 F_X. \quad (3.7)$$

Its expectation value  $F_X$  sets the scale of SUSY breaking as  $\sqrt{F_X}$ . The other expectation value  $M$  gives each messenger fermion a mass  $M$ , and the scalars mass squared masses

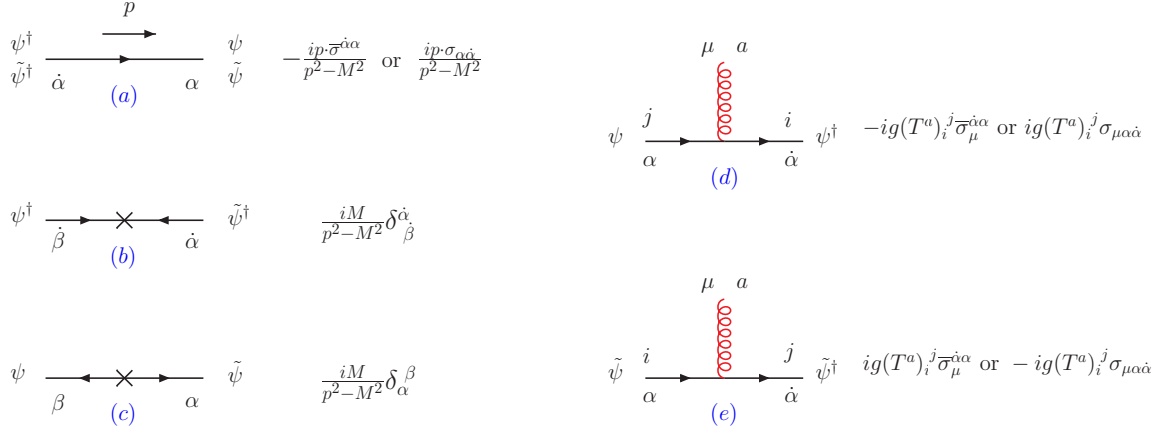


**Figure 2.** The Feynman rules for the messenger fermions

equal to  $M^2 \pm F_X$ . The corresponding mass eigenstates of the scalars are given in terms of the gauge eigenstates of the scalars as follows:

$$\begin{pmatrix} \phi_- \\ \phi_+ \end{pmatrix} = \frac{1}{\sqrt{2}} \begin{pmatrix} 1 & 1 \\ 1 & -1 \end{pmatrix} \begin{pmatrix} \phi \\ \tilde{\phi}^\dagger \end{pmatrix}. \quad (3.8)$$

For the Feynman rules we select the mass eigenstates for the messenger scalars.

### 3.2 Feynman rules

In order to systematically perform perturbative calculations we first establish a set of Feynman rules for the MGM using the two-component spinor formalism. Following the conventions for the Feynman rules in ref. [19] we acquire them as depicted in figure 2, 3, 4, and 5. Here we use the usual Feynman gauge for the gluon field. We omit the Feynman rules for the gluon for the sake of saving space.

The messenger fermions have four different propagators: the two are chirality-preserving as shown in figure 2 (a) while the other two chirality-violating as shown in figure 2 (b) and (c). For the Feynman rules for chirality-preserving propagators we have two options for them: either  $\bar{\sigma}$  or  $\sigma$ . For the Feynman rules for fermion-fermion-gluon vertices we can also select either  $\bar{\sigma}$  or  $\sigma$  as shown in figure 2 (d) and (e). But the choice on  $\sigma$  matrices for propagators and the vertices in a Feynman diagram should be simultaneously fixed. For instance, if one chooses a  $\sigma$  for a propagator then its neighboring vertices must pick out a  $\bar{\sigma}$ .

As for a gluino we have only a chirality-preserving propagator as shown in figure 3 because it is massless. The gluino propagator as well as the gluino-gluino-gluon vertex can contain either  $\bar{\sigma}$  or  $\sigma$  like the messenger fermions.

The messenger scalars have two different four-vertices which are obtained by integrating out  $\mathcal{D}^a$ -term in Eq. (3.2): the same mass eigenstates have *either* the same directions of their arrows as shown in figure 4 (d) *or* the opposite directions of their arrows as shown in figure 4 (e).

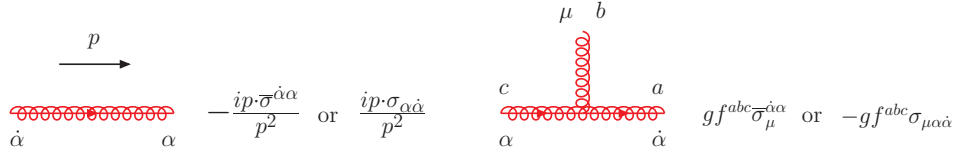


**Figure 3.** The Feynman rules for the gluino

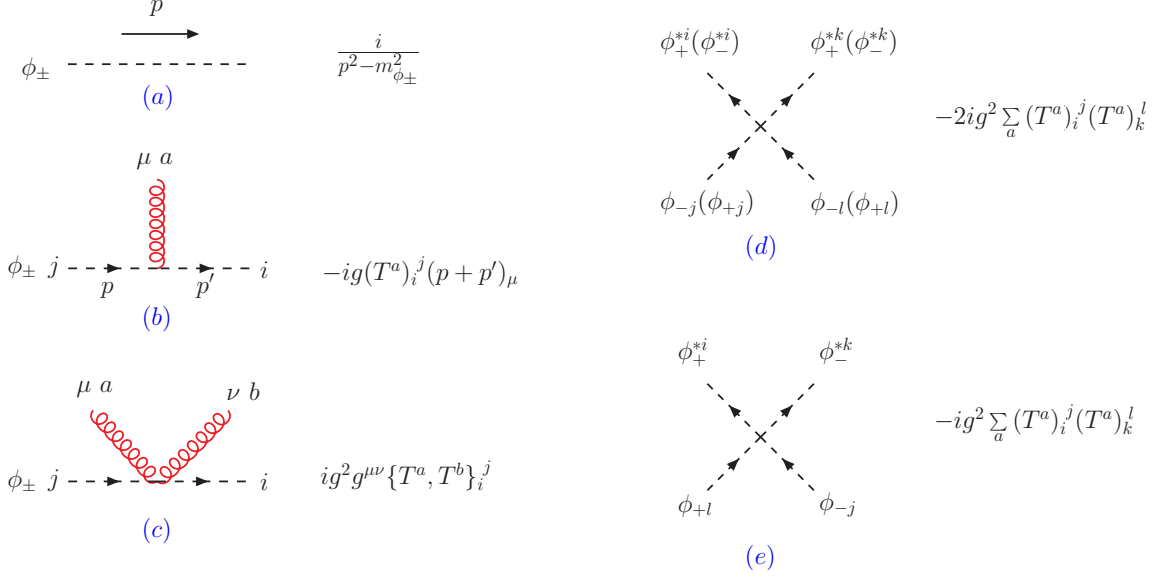


**Figure 4.** The Feynman rules for the messenger scalars

There are eight different scalar-fermion-gluino three-vertices as shown in figure 5. One should pay attention to every direction of arrows of fields in the vertex diagrams. There are some important properties to recall:

- A direction of arrow of a messenger fermion ( $\psi$  or  $\tilde{\psi}$ ) is the same as that of gluino: either into a vertex or out of a vertex.
- A direction of arrow of a messenger scalar is *either* the same with that of a messenger fermion  $\tilde{\psi}$  *or* the opposite with that of the messenger fermion  $\psi$ .
- Among the eight vertices only the two in figure 5 (d) and (f) have a positive sign in the Feynman rules while the rest a negative sign.

Although we do not include the MSSM quarks and squarks in the lagrangian (3.2) we need to take account of their effects on the renormalization procedure for later numerical analysis. Here we omit their Feynman rules which are referred to in ref. [19].

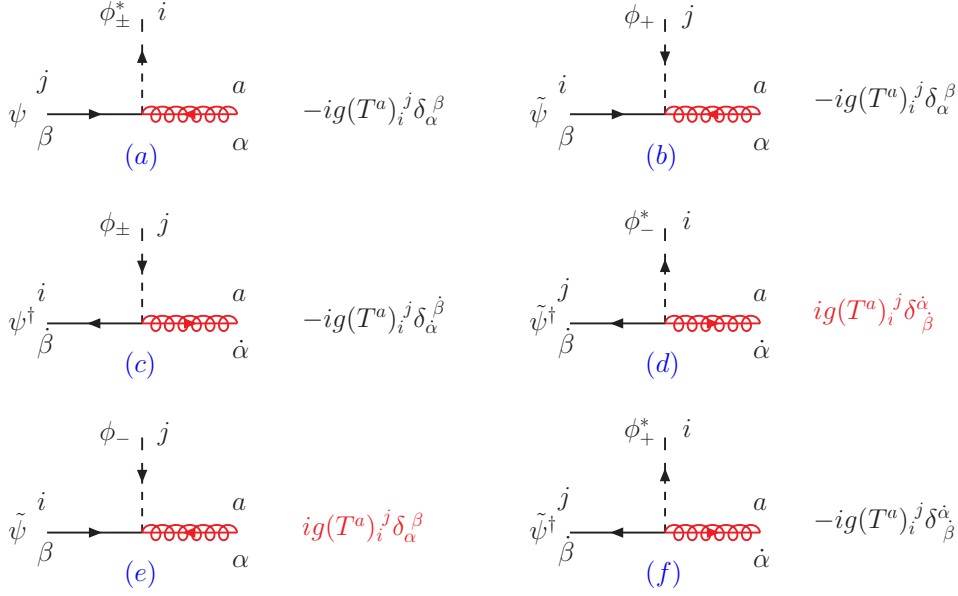


**Figure 5.** The Feynman rules for the scalar-fermion-gluino vertices.

## 4 Renormalization

We shall perform loop calculations for the self-energy and vertex functions using the Feynman rules as described in the previous section. We consider the one-loop and counterterm corrections to the propagators and vertices relevant for the gluino pole mass. As mentioned earlier we take into account the MSSM quarks and squarks whose propagators appear in the loops of figure 6, 7, and 13.

All the corrections for the propagators are depicted in figure 6, 7, 8, 9, 10, and 11:

- Figure 6 shows the one-loop and counterterm corrections to the gluino propagator. The solid lines represent either the messenger fermions or quarks while the dashed lines either the messenger scalars or squarks. The second to the last denotes the ghost loop corrections while the last stands for the counterterm.
- Figure 7 shows the one-loop and counterterm corrections to the chirality-preserving gluino propagator. There are four different combinations of the messenger fermions and messenger scalars in the loop and their contributions are constructive, leading to  $UV$  divergence. We include not only the messenger fermion-scalar loops but also the quark-squark loops.
- Figure 8 shows the one-loop corrections to the chirality-violating gluino propagator. There are four different combinations of the messenger fermions and messenger scalars in the loop but their contributions are destructive, resulting in no counterterm. They yield the pole mass of the gluino at one-loop order.
- Figure 9 shows the one-loop and counterterm corrections to the chirality-preserving messenger fermion propagator.



- Figure 10 shows the one-loop and counterterm corrections to the chirality-violating messenger fermion propagator.
- Figure 11 shows the one-loop and counterterm corrections to the messenger scalar propagator.

All the corrections to the three-vertices are depicted in figure 12, 13, 14, and 15:

- Figure 12 shows the one-loop and counterterm corrections to the messenger scalar-messenger scalar-gluon vertex. Reversing the arrow direction of either the messenger fermion or gluino is also taken into account.
- Figure 13 shows the one-loop and counterterm corrections to the gluino-gluino-gluon vertex. We include not only the messenger fermion-scalar loops but also the quark-squark loops.
- Figure 14 shows the one-loop and counterterm corrections to the messenger fermion-messenger fermion-gluon vertex.
- Figure 15 shows the one-loop and counterterm corrections to the messenger fermion-messenger scalar-gluino vertex.

The  $\overline{\text{DR}}$  scheme treats the UV divergences in the same way as the  $\overline{\text{MS}}$  scheme. The main difference between the two schemes is that degrees of freedom of a chiral fermion field in the  $\overline{\text{DR}}$  scheme are set to 2 while those in the  $\overline{\text{MS}}$  scheme to  $d/2$ . Therefore gauge fields in the  $\overline{\text{DR}}$  scheme are accompanied by the  $\varepsilon$ -scalar fields to maintain supersymmetry. At one-loop order, it is equivalent to set the dimensions in which the  $\sigma$  matrices reside to 2.

The renormalization  $Z$  factors are defined as

$$Z = 1 + \left( \frac{\alpha_s}{4\pi} \right) \frac{Z^{(1)}}{\varepsilon} + \mathcal{O}(\alpha_s^2), \quad (4.1)$$

and cancel off the inverse powers of  $\varepsilon$  of the one-loop integrals in the figures. Both the one-loop corrections to the propagators and vertices yield the leading term of power series in  $\alpha_s$  for  $Z^{(1)}$ 's. We list them in figure 16 and 17 where  $N_f$  is the number of MSSM quark flavor and  $N_{\text{mess}}$  is the number of the messenger pairs. The Casimir operators  $C(R)$ ,  $C_2(R)$  and  $C_2(G)$  are defined as

$$(\mathbf{T}^a \mathbf{T}^a)_i^j = C_2(R) \delta_i^j \quad (4.2)$$

$$\text{Tr}[\mathbf{T}^a \mathbf{T}^b] = C(R) \delta^{ab} \quad (4.3)$$

$$f^{acd} f^{bcd} = C_2(G) \delta^{ab}, \quad (4.4)$$

whose values are  $C(R) = 1/2$ ,  $C_2(R) = 4/3$  and  $C_2(G) = 3$  for the  $SU(3)_C$  gauge symmetry, respectively.

As a consistency check we evaluate *Slavnov-Taylor* identities,

$$Z_g = \frac{Z_{\psi\psi v}}{Z_\psi \sqrt{Z_v}} = \frac{Z_{\phi\phi v}}{Z_\phi \sqrt{Z_v}} = \frac{Z_{\lambda\lambda v}}{Z_\lambda \sqrt{Z_v}} = \frac{Z_{\psi\phi v}}{\sqrt{Z_\psi} \sqrt{Z_\phi} \sqrt{Z_v}} = \frac{Z_{vvv}}{\sqrt{Z_v^3}}, \quad (4.5)$$

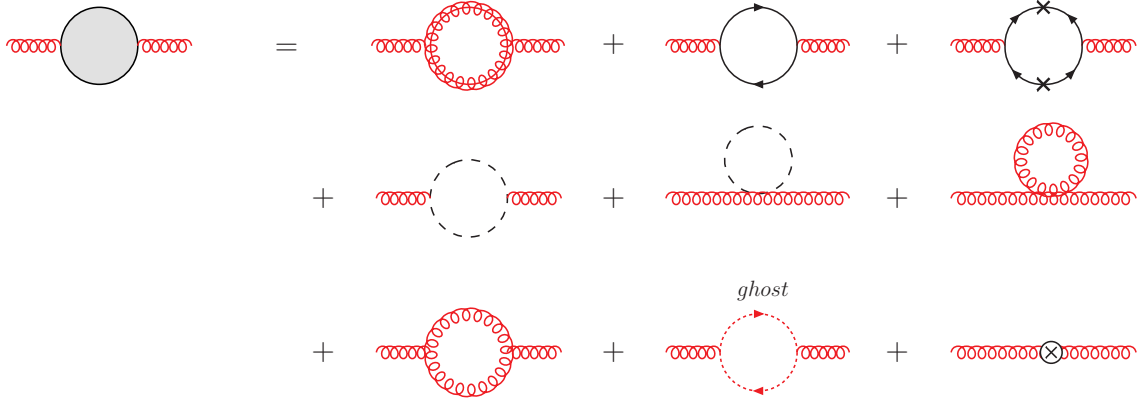


**Figure 6.** The one-loop and counterterm corrections to the gluon propagator.



**Figure 7.** The one-loop and counterterm corrections to the chirality-preserving gluino propagator.



**Figure 8.** The one-loop corrections to the chirality-violating gluino propagator. They contribute to the pole mass of the gluino at one-loop order.



**Figure 9.** The one-loop and counterterm corrections to the chirality-preserving messenger fermion propagator.

where the various  $Z$  factors are calculated at one-loop order. We obtain the leading coefficient of the renormalization  $Z$  factor for the gauge coupling,

$$Z_g^{(1)} = -\frac{3}{2}C_2(G) + (N_f + N_{\text{mess}})C(R). \quad (4.6)$$

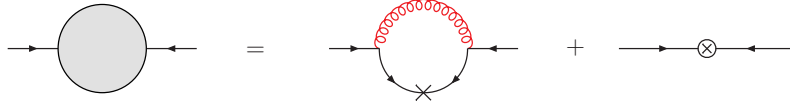


**Figure 10.** The one-loop and counterterm corrections to the chirality-violating messenger fermion propagator.

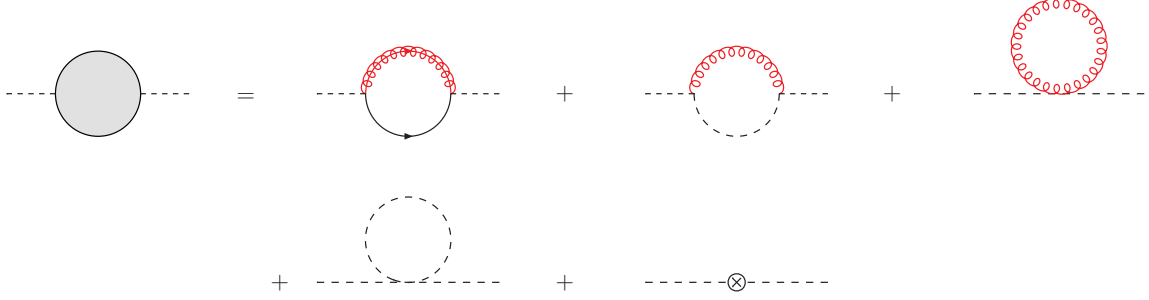


**Figure 11.** The one-loop and counterterm corrections to the messenger scalar propagator.

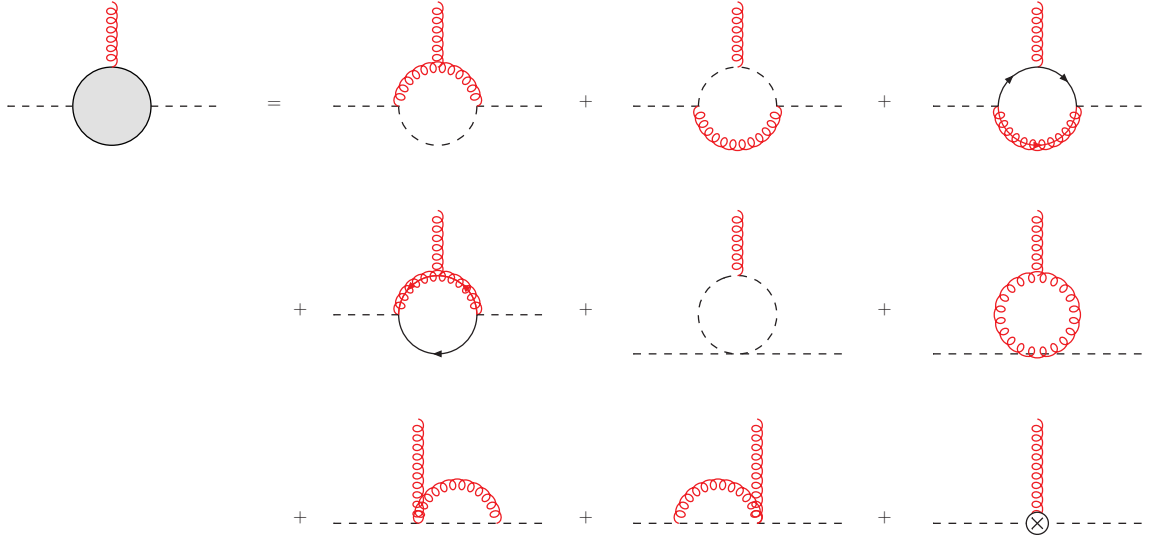


**Figure 12.** The one-loop and counterterm corrections to the messenger scalar-messenger scalar-gluon vertex.

## 5 Self-energy functions

### 5.1 Self-energy functions at one-loop order

We first calculate the helicity-conserving self-energy function  $\Omega^{(1)}$  which arises from the one-loop diagrams as shown in figure 8. The sum of the four different configurations in the internal loops is free from UV and IR divergence, yielding the gluino pole mass at one-loop

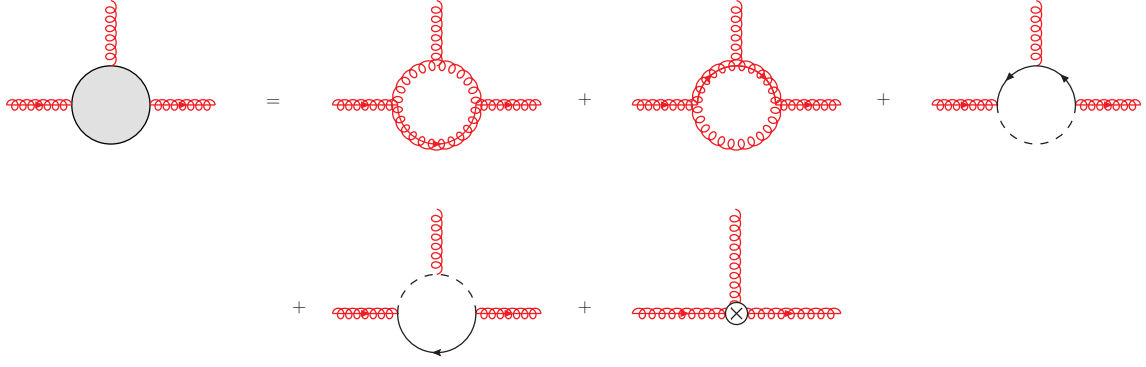


**Figure 13.** The one-loop and counterterm corrections to the gluino-gluino-gluon vertex.

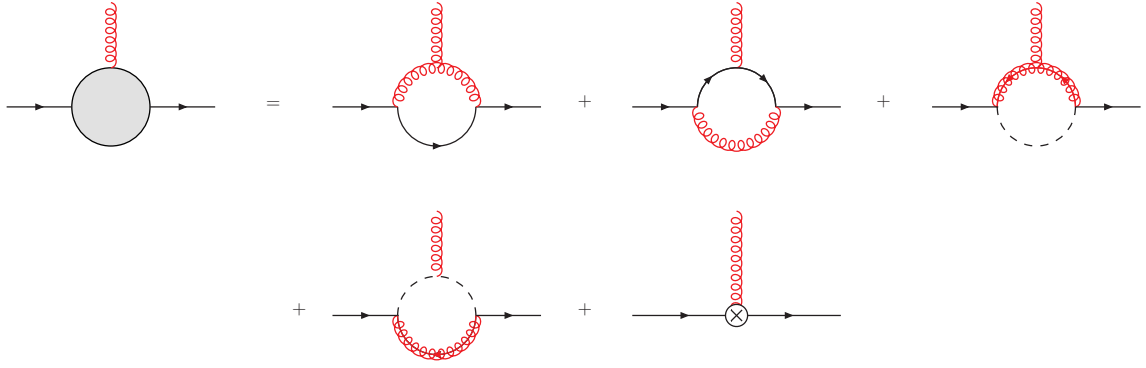


**Figure 14.** The one-loop and counterterm corrections to the messenger fermion-messenger fermion-gluon vertex.

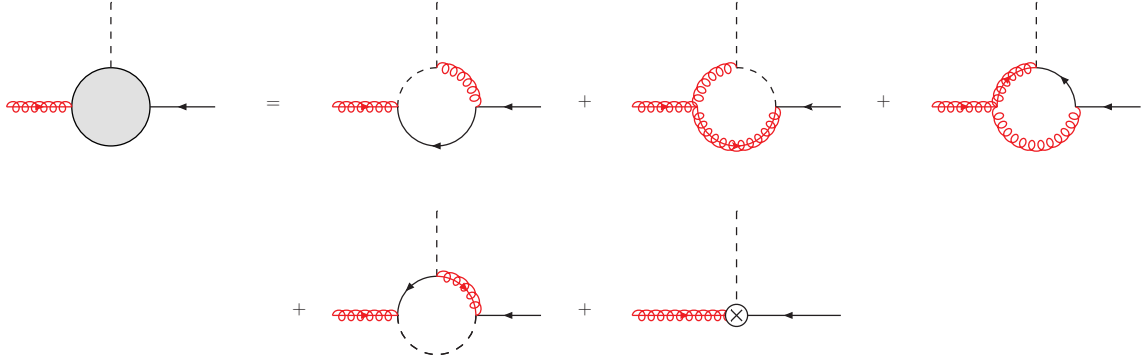


**Figure 15.** The one-loop and counterterm corrections to the messenger scalar-messenger fermion-gluon vertex.

order as,

$$\begin{aligned}
 \sqrt{s} &= m_{\tilde{g}} = \Omega^{(1)}(s) \\
 &= 2N_{\text{mess}}M_{\text{mess}}\left(\frac{\alpha_s}{4\pi}\right)C(R)\left(-(\eta_1-1)\ln(\eta_2x+1)-(\eta_2-1)\ln(\eta_1x+1)-(r\leftrightarrow\tilde{r})\right),
 \end{aligned}
 \tag{5.1}$$

$$\begin{aligned}
\begin{array}{c} \xrightarrow{p} \\ \text{---} \otimes \text{---} \end{array} &= ip \cdot \bar{\sigma}(Z_\psi - 1), & Z_\psi^{(1)} &= -2C_2(R) \\
\begin{array}{c} \xrightarrow{p} \\ \text{---} \otimes \text{---} \end{array} &= -iM(Z_\psi Z_M - 1), & Z_M^{(1)} &= -2C_2(R) \\
\begin{array}{c} \xrightarrow{p} \\ \text{---} \otimes \text{---} \end{array} &= i[p^2(Z_\phi - 1) - M^2(Z_\phi Z_M^2 - 1) \mp F_X(Z_\phi Z_{F_X} - 1)], & Z_\phi^{(1)} &= 0, \quad Z_{F_X}^{(1)} = -2C_2(R) \\
\begin{array}{c} \xrightarrow{p} \\ \text{---} \otimes \text{---} \end{array} &= i(p_\mu p_\nu - p^2 g_{\mu\nu})(Z_v - 1), & Z_v^{(1)} &= C_2(G) - 2(N_f + N_{\text{mess}})C(R) \\
\begin{array}{c} \xrightarrow{p} \\ \text{---} \otimes \text{---} \end{array} &= ip \cdot \bar{\sigma}(Z_\lambda - 1), & Z_\lambda^{(1)} &= -C_2(G) - 2(N_f + N_{\text{mess}})C(R)
\end{aligned}$$

**Figure 16.** The counterterm corrections to the propagators.

$$\begin{aligned}
\begin{array}{c} \mu \\ \text{---} \otimes \text{---} \\ j \text{---} \text{---} i \end{array} &= -ig(T^a)_i^j \bar{\sigma}_\mu(Z_{\psi\psi v} - 1), & Z_{\psi\psi v}^{(1)} &= -C_2(G) - 2C_2(R) \\
\begin{array}{c} \mu \\ \text{---} \otimes \text{---} \\ j \text{---} p \text{---} p' \text{---} i \end{array} &= -ig(T^a)_i^j (p_\mu + p'_\mu)(Z_{\phi\phi v} - 1), & Z_{\phi\phi v}^{(1)} &= -C_2(G) \\
\begin{array}{c} \mu \\ \text{---} \otimes \text{---} \\ c \text{---} \text{---} a \end{array} &= gf^{abc} \bar{\sigma}_\mu(Z_{\lambda\lambda v} - 1), & Z_{\lambda\lambda v}^{(1)} &= -2C_2(G) - 2(N_f + N_{\text{mess}})C(R) \\
\begin{array}{c} i \\ \text{---} \otimes \text{---} \\ j \text{---} \text{---} a \end{array} &= -ig(T^a)_i^j (Z_{\psi\phi\lambda} - 1), & Z_{\psi\phi\lambda}^{(1)} &= -2C_2(G) - C_2(R)
\end{aligned}$$

**Figure 17.** The counterterm corrections to the vertices.

where

$$x = -\frac{p^2}{M_{\text{mess}}^2} = -\frac{s}{M_{\text{mess}}^2}, \quad (5.2)$$

$$r = \frac{m_{\phi+}^2}{M_{\text{mess}}^2} = 1 + \frac{\Lambda}{M_{\text{mess}}}, \quad (5.3)$$

$$\tilde{r} = \frac{m_{\phi-}^2}{M_{\text{mess}}^2} = 1 - \frac{\Lambda}{M_{\text{mess}}}, \quad (5.4)$$

$$\eta_{1,2} = \frac{r+x-1}{2x} \pm \frac{1}{2x} \sqrt{r^2 + 2r(x-1) + (x+1)^2}, \quad (5.5)$$

and  $p^\mu$  is the external four momentum.  $M_{\text{mess}}$  is messenger fermion mass (which is denoted by  $M$  in section 3) and  $\Lambda$  is SUSY breaking scale of the visible sector which is equivalent to  $F_X/M_{\text{mess}}$ . It is noted that the self-energy function  $\Omega^{(1)}$  has no explicit dependence on the renormalization scale,  $\mu$ . Since the relevant range of  $s$  is much lower than the messenger scale, *i.e.*  $x \leq 10^{-4}$ , it is a good approximation to take the limit  $x \rightarrow 0$ . Then  $\Omega^{(1)}$  is given by [20, 21],

$$\Omega^{(1)}(s)|_{x \rightarrow 0} = \left(\frac{\alpha_s}{4\pi}\right) \Lambda N_{\text{mess}} 2C(R) \left[ \frac{r \ln(r)}{(r-1)^2} + (r \leftrightarrow \tilde{r}) \right]. \quad (5.6)$$

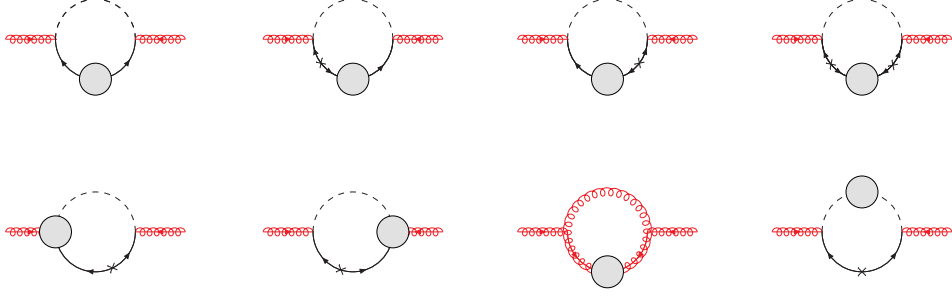


**Figure 18.** The two-loop contributions to the chirality-violating gaugino propagator. Each shaded circle denotes the one-loop and counterterm corrections either to the propagators or to the vertices. The dashed line can be either  $\phi_+$  or  $\phi_-$  while the solid line either  $\psi$  or  $\tilde{\psi}$ .

The helicity-violating self-energy function  $\Xi^{(1)}$ , stemming from the diagrams in figure 7, is given as

$$\begin{aligned} \Xi^{(1)}(s) = & \left( \frac{\alpha_s}{4\pi} \right) C(R) \left[ -N_{\text{mess}} \left( \left( (\eta_1 - 1) \ln(\eta_2 x + 1) + (\eta_2 - 1) \ln(\eta_1 x + 1) \right) \left( \frac{r + x - 1}{x} \right) \right. \right. \\ & + 2 + \frac{r - 1}{x} + \frac{r \ln(r)}{x} + \ln \left( \frac{\mu^2}{M_{\text{mess}}^2} \right) + (r \leftrightarrow \tilde{r}) \left. \right) + 2N_f \left( \ln \left( \frac{-s}{\mu^2} \right) - 2 \right) \Big] \\ & + \left( \frac{\alpha_s}{4\pi} \right) C_2(G) \left[ \ln \left( \frac{-s}{\mu^2} \right) - 2 \right]. \end{aligned} \quad (5.7)$$

As mentioned earlier, it consists of the three parts: (i) the messenger loops, (ii) the quark-squark loops, and (iii) the gluino-gluon loops. In the limit  $x \rightarrow 0$ , it is reduced to

$$\begin{aligned} \Xi^{(1)}(s)|_{x \rightarrow 0} = & \left( \frac{\alpha_s}{4\pi} \right) \left[ C(R) \left( N_{\text{mess}} \left( \frac{r \ln(r)}{r - 1} + \frac{\tilde{r} \ln(\tilde{r})}{\tilde{r} - 1} - 2 - 2 \ln \left( \frac{\mu^2}{M_{\text{mess}}^2} \right) \right) \right. \right. \\ & \left. \left. + 2N_f \left( \ln \left( \frac{-s}{\mu^2} \right) - 2 \right) \right) + C_2(G) \left( \ln \left( \frac{-s}{\mu^2} \right) - 2 \right) \right]. \end{aligned} \quad (5.8)$$

We will comment on the IR behavior in  $\Xi^{(1)}(s)$  in the next subsection.

## 5.2 Self-energy function at two-loop order

In this section we describe how to calculate the self-energy function  $\Omega^{(2)}(s)$  in detail. All the Feynman diagrams relevant to  $\Omega^{(2)}$  are shown in figure 18, where each shaded circle denotes the one-loop and counterterm corrections either to the propagators or to the vertices in Section 4. The sum of the Feynman diagrams contains no UV divergence due to the inclusion of the counterterm corrections at one-loop level.

We take a few steps to calculate the Feynman diagrams. We first decompose a Feynman integral with momentum tensors in numerators into integral forms of scalar products using the Gram determinant. Reducing the scalar Feynman integrals to the master integrals we use Laporta's algorithm [22], which systematically applies several reduction methods, such as Passarino-Veltman reduction [23], integration-by-part method [24, 25] and Lorentz

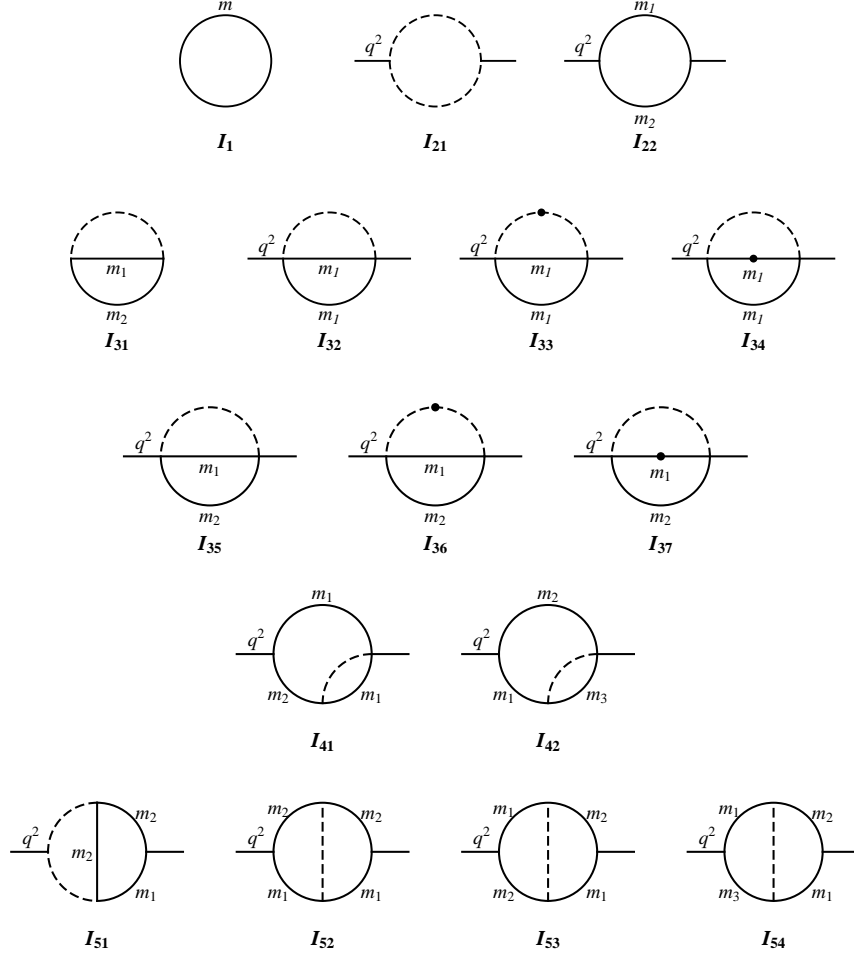


**Figure 19.** The master integrals. A dashed line represents a massless propagator while a solid line a massive propagator whose mass is explicitly noted. A dot on a solid(dashed) line denotes a double propagator.

invariance method [26]. All the reduction procedures have been executed with our in-house Mathematica code.

The *sixteen* master integrals are cataloged in figure 19. The dashed lines represent massless propagators while the solid lines massive propagators whose masses are explicitly noted. A dot on a solid(dashed) line denotes a double propagator. To evaluate the master integrals we mainly use the Mellin-Barnes representation which is described in ref. [27]. The analytic forms of the master integrals are fully described in appendix A.

Performing all the procedures we acquire the self-energy function  $\Omega^{(2)}(s)$ . We checked that all the UV divergent poles exactly cancel out. The complete form of  $\Omega^{(2)}(s)$  is so lengthy that it is attached in Appendix B. In the limit  $x \rightarrow 0$ , the explicit formula of  $\Omega^{(2)}$

is approximated by,

$$\begin{aligned}
\Omega^{(2)}(s)|_{x \rightarrow 0} = & \left( \frac{\alpha_s}{4\pi} \right)^2 \Lambda N_{\text{mess}} 2C(R) \left[ C_2(G) \left( \frac{\ln(r)}{(r-1)^2} \left( 8r - 4r \ln \left( \frac{-s}{\mu^2} \right) \right. \right. \right. \\
& + \left. \left. \left( 2r + \frac{1}{r-1} \right) \ln(r) + \ln(\tilde{r}) \right) + \frac{4r-2}{(r-1)^2} \text{Li}_2(1-r) + \frac{2}{r-1} \text{Li}_2 \left( \frac{2r-2}{r} \right) \right) \\
& + C_2(R) \frac{\ln(r)}{(r-1)^2} \left( 6r + 2 + 2(r+1) \ln \left( \frac{\mu^2}{M_{\text{mess}}^2} \right) - \frac{r(r-3)}{r-1} \ln(r) + \ln(\tilde{r}) \right) \\
& \left. + (r \leftrightarrow \tilde{r}) \right]. \tag{5.9}
\end{aligned}$$

The first three diagrams (from left to right) on the second row shown in figure 18 contribute to the term proportional to  $C_2(G)$  in Eq. (5.9) while all the diagrams except for the one at the intersection of the second row and third column contribute to the term proportional to  $C_2(R)$  in Eq. (5.9). The term proportional to  $C_2(G)$  contains a term that represents IR behavior, *i.e.*  $\ln(-s/\mu^2)$ , since the gluon and gluino in the propagators are massless. On the other hand, the term proportional to  $C_2(R)$  have an large logarithm,  $\ln(\mu^2/M_{\text{mess}}^2)$ , since we take the renormalization scale  $\mu$  as the physical gluino mass scale.

As a side note we comment on the large logarithm,  $\ln(\mu^2/M_{\text{mess}}^2)$ , in both  $\Xi^{(1)}(s)$  and  $\Omega^{(2)}(s)$ . For  $N_{\text{mess}} = 1$  the term with  $\ln(\mu^2/M_{\text{mess}}^2)$  in  $\Xi^{(1)}(s)$  gives less than 0.2 even though the  $M_{\text{mess}}$  goes up to  $10^5$  TeV due to the small coupling constant  $\alpha_s/(4\pi) = 0.008$  at  $\mu \sim 1$  TeV. Therefore we can safely do perturbation for the computation of the pole mass. However, this term increases linearly with  $N_{\text{mess}}$ . For the case  $N_{\text{mess}} \geq 3$  with large  $M_{\text{mess}}$ , it is required to resum this large logarithmic term in order to make perturbative expansion valid. As for the  $\ln(\mu^2/M_{\text{mess}}^2)$  term in  $\Omega^{(2)}(s)$ , we emphasize that the coefficient of this logarithm turns out to be much smaller than the other terms for a broad range of the value  $r$ . Especially in the large messenger mass limit this term vanishes. Therefore the resummation of the large logarithm is expected to be negligible in  $\Omega^{(2)}$ .

In order to investigate characteristics of the self-energy functions we consider their behavior in a large messenger mass limit ( $x \rightarrow 0$  and  $M_{\text{mess}} \gg \sqrt{F_X}$ ). In this limit, they become

$$\Omega^{(1)}(s) = \left( \frac{\alpha_s}{4\pi} \right) \Lambda N_{\text{mess}} 2C(R), \tag{5.10}$$

$$\Omega^{(2)}(s) = \left( \frac{\alpha_s}{4\pi} \right)^2 \Lambda N_{\text{mess}} 2C(R) C_2(G) \left( 9 - 4 \ln \left( \frac{-s}{\mu^2} \right) \right), \tag{5.11}$$

$$\begin{aligned}
\Xi^{(1)}(s) = & \left( \frac{\alpha_s}{4\pi} \right) \left[ C(R) \left( 2N_f \left( \ln \left( \frac{-s}{\mu^2} \right) - 2 \right) \right. \right. \\
& \left. \left. - 2N_{\text{mess}} \ln \left( \frac{\mu^2}{M_{\text{mess}}^2} \right) \right) + C_2(G) \left( \ln \left( \frac{-s}{\mu^2} \right) - 2 \right) \right]. \tag{5.12}
\end{aligned}$$

Eq. (5.10) is the well known result used in various literatures for the gluino mass at one-loop order. As for  $\Omega^{(2)}$  the large logarithm term does not appear in Eq. (5.11) as mentioned



above. It should be noted that the factor 9 in Eq. (5.11) is much greater than 2 which are shown in Eq. (12) of ref. [15]. It turns out that the difference between the factor 9 and 2 originates from different treatments of IR behavior. This large factor, as shown in the next section, leads to a significant enhancement to the gluino pole mass at two-loop order compared with the result in ref. [15]. We retain an IR behavior in the self-energy functions at two-loop order while the authors in ref. [15] get rid of an IR divergence. Since the IR behavior persists in the self-energy functions  $\Omega^{(2)}$  and  $\Xi^{(1)}$  it is appropriate to keep an IR dependence on the gluino pole mass at two-loop order. In this regards, our method for the gluino pole mass at two-loop order is more consistent with perturbation theory rather than that of ref. [15].

## 6 Numerical Analysis

In this section we perform a numerical analysis of the gluino pole mass using the three self-energy functions in Section 5. In order to illustrate the numerical significance of the NLO correction to the gluino pole mass we compare the NLO pole mass with the LO pole mass. The strong coupling constant within the standard model is given as  $\alpha_s(m_Z) = 0.118$ , and the  $Z$ -boson mass is given as  $m_Z = 91.187$  GeV, and the top quark mass is given by  $m_t = 173.1$  GeV. The top quark mass is required for the  $\alpha_s$  running. The final  $\overline{\text{DR}}$  values of the gauge coupling  $\alpha_s$  and of the fermion masses can be converted into the  $\overline{\text{MS}}$  ones at one-loop order <sup>3</sup> using

$$\alpha_s^{\overline{\text{MS}}} = \alpha_s^{\overline{\text{DR}}} \left( 1 - \frac{\alpha_s^{\overline{\text{DR}}}}{4\pi} \frac{C_2(G)}{3} \right), \quad (6.1)$$

$$M^{\overline{\text{MS}}} = M^{\overline{\text{DR}}} \left( 1 + \frac{\alpha_s^{\overline{\text{DR}}}}{4\pi} C_2(G) \right). \quad (6.2)$$

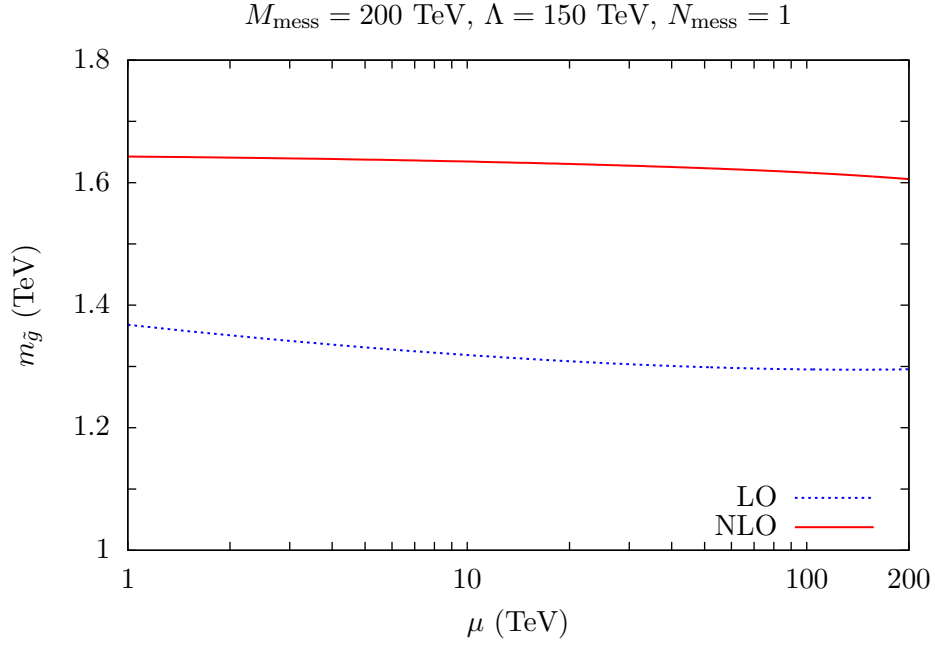
Figure 20 shows that the renormalization-scale dependence of the LO and NLO pole mass of the gluino, for  $\Lambda = 150$  TeV,  $M_{\text{mess}} = 200$  TeV and  $N_{\text{mess}} = 1$ . The LO contribution to the pole mass has no explicit dependence on the renormalization scale  $\mu$ . But the introduction of the running gauge coupling brings about the renormalization-scale dependence on the LO pole mass. Thus the LO pole mass decreases as the renormalization scale increases. The scale dependence of gluino pole mass is alleviated at the NLO.

Figure 21 compares the LO and NLO pole mass of the gluino as a function of the messenger mass  $M_{\text{mess}}$ , for  $\mu = 1$  TeV,  $\Lambda = 150$  TeV and  $N_{\text{mess}} = 1$ . For a fixed visible supersymmetry breaking scale, both the LO and NLO pole masses are saturated and the NLO correction barely changes as the messenger mass scale increases.

Figure 22 shows both the LO and NLO pole masses increase as the visible supersymmetry breaking scale increases for a fixed messenger mass scale. The NLO correction to pole mass also monotonically increases as  $M_{\text{mess}}$  increases for fixed values of  $\mu$  and  $\Lambda$ . All in all, the NLO correction to pole mass is roughly 20% of the LO pole masses of the gluino among the three plots.

---

<sup>3</sup>The relations between  $\overline{\text{DR}}$  and  $\overline{\text{MS}}$  schemes at two- and three-loop order are given in ref. [28] and [29].



**Figure 20.** The renormalization scale-dependence of the LO (dashed line) and NLO (solid line) pole masses of the gluino for  $\Lambda = 150 \text{ TeV}$ ,  $M_{\text{mess}} = 200 \text{ TeV}$  and  $N_{\text{mess}} = 1$ .

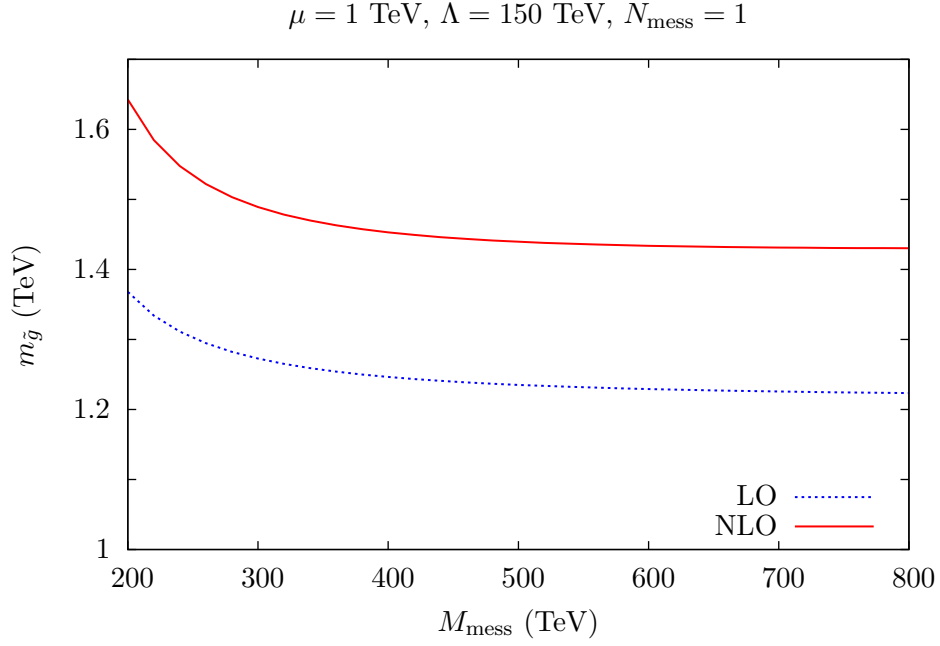


**Figure 21.** The messenger scale-dependence of the LO (dashed line) and NLO (solid line) pole masses of the gluino for  $\mu = 1 \text{ TeV}$ ,  $\Lambda = 150 \text{ TeV}$  and  $N_{\text{mess}} = 1$ .

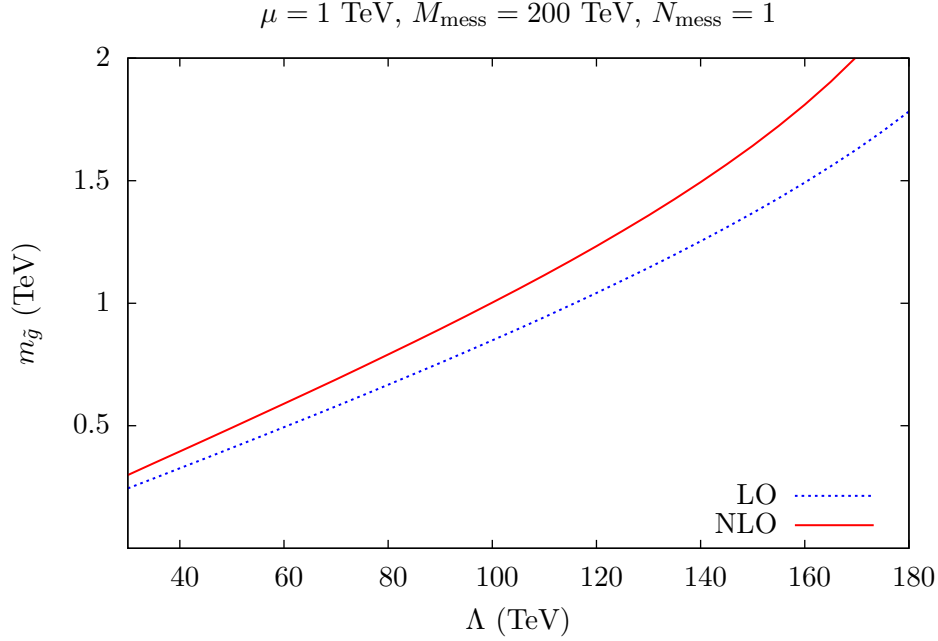


**Figure 22.** The SUSY breaking scale-dependence of the LO (dashed line) and NLO (solid line) pole mass for  $\mu = 1 \text{ TeV}$ ,  $M_{\text{mess}} = 200 \text{ TeV}$  and  $N_{\text{mess}} = 1$ .

We consider benchmark planes, lines and points of the MGM in order to interpret the experimental results in terms of possible manifestations of SUSY. The authors in ref. [30] proposed the benchmark planes, lines and points of the mGMSB model, producing the spectra at specific benchmark points that illustrate different possible experimental signatures. We adopt their benchmark points and calculate the ratio of the NLO pole mass correction to the LO pole mass. Table 1 shows the benchmark points along the benchmark line,  $m\text{GMSB1}$  which is defined by  $N_{\text{mess}} = 3, \tan \beta = 15, \mu > 0, \Lambda = M_{\text{mess}}/2$  with  $\Delta M_{\text{mess}} = 10 \text{ TeV}$ . Table 2 lists the benchmark point along the benchmark line,  $m\text{GMSB2.1}$  which is defined by  $N_{\text{mess}} = 1, \tan \beta = 15, \mu > 0, \Lambda = 0.9 M_{\text{mess}}$  with  $\Delta M_{\text{mess}} = 10 \text{ TeV}$ . We see that the ratio of the NLO pole mass correction to the LO pole mass for the gluino can reach 32% in the  $m\text{GMSB1}$ . The large ratio compared with that of the  $m\text{GMSB2.1}$  is mainly due to  $N_{\text{mess}}^2$  in the  $\Omega^{(1)}\Xi^{(1)}$ .

All the numerical analyses indicate that the NLO correction is large enough to reach 20% of the LO pole mass or even more. There are three ingredients for the large correction: (i) the relative strength of the  $SU(3)_C$  gauge coupling is large, (ii) the color representation of the gluino is octet, (iii) and the number of the Feynman diagrams associated with the messenger fields are large. The first two reasons are same with that of gravity mediation mechanism (*i.e.* CMSSM) while the last is characteristic of gauge mediation mechanism.

Points	$M_{\text{mess}}/\text{TeV}$	$m_{\tilde{g}}^{LO}$	$m_{\tilde{g}}^{NLO}$	$\Delta m_{\tilde{g}}/m_{\tilde{g}}^{LO}$
mGMSB1.1	70	953	1256	0.32
mGMSB1.2	80	1089	1436	0.32
mGMSB1.3	90	1225	1616	0.32
mGMSB1.4	100	1361	1796	0.32
mGMSB1.5	110	1497	1977	0.32
mGMSB1.6	120	1633	2157	0.32

**Table 1.** Line mGMSB1:  $N_{\text{mess}} = 3, \tan \beta = 15, \mu > 0, \Delta M_{\text{mess}} = 10 \text{ TeV}$  (masses in GeV).

Points	$M_{\text{mess}}/\text{TeV}$	$m_{\tilde{g}}^{LO}$	$m_{\tilde{g}}^{NLO}$	$\Delta m_{\tilde{g}}/m_{\tilde{g}}^{LO}$
mGMSB2.1.1	80	719	917	0.275
mGMSB2.1.2	90	809	1031	0.275
mGMSB2.1.3	100	898	1145	0.275
mGMSB2.1.4	110	988	1259	0.274
mGMSB2.1.5	120	1078	1373	0.274
mGMSB2.1.6	130	1168	1488	0.274

**Table 2.** Line mGMSB2.1:  $N_{\text{mess}} = 1, \tan \beta = 15, \mu > 0, \Lambda = 0.9 M_{\text{mess}}$  with  $\Delta M_{\text{mess}} = 10 \text{ TeV}$  (masses in GeV).

## 7 Conclusion and Outlook

We have presented the self-energy functions for the gluino of the minimal gauge mediation at two-loop order and studied the radiative corrections on the gluino pole mass. The one-loop pole mass is the leading order while the two-loop correction is the next-to-leading order. The next-to-leading order correction shifts the leading order pole mass by roughly 20% or even more. This shift is much larger than the expected accuracy of the mass determination at the LHC, and should be reckoned with for precision studies on the SUSY breaking parameters.

Not only the gluino mass but also the squark masses are crucial to study the phenomenology at the LHC. The squark masses also involve the SUSY QCD so that its contribution from higher order radiative corrections are expected to be large. The numerical significance of the next-to-leading corrections to the squark masses deserves a detailed investigation which we leave for future study.

The next-to-lightest-superstmmetric particle (NLSP) in gauge mediation is mostly either neutralino or stau depending on the specific regions in parameter space. Using the full expressions of the self-energy functions one can evaluate the significance of the radiative corrections for the NLSP mass and refine the spectra at the benchmark points of the minimal gauge mediation model.

In this paper we have focused only on the minimal gauge mediation. Other gauge mediation models tend to retain the feature that the higher order radiative corrections to the gluino pole mass are substantial. Thus when one quantitatively studies complicated

SUSY-breaking models associated with gauge mediation one must pay attention to the next-to-leading order or higher order radiative corrections to the gluino mass in addition to the leading order result.

## Acknowledgments

J.Y. Lee and Y.W. Yoon are supported by Basic Science Research Program through the National Research Foundation of Korea(NRF) funded by the Ministry of Education, Science and Technology(2011-0003974). J.Y. Lee is also supported partially by Mid-career Research Program through the NRF grant funded by the MEST(2011-0027559). Y.W. Yoon thanks KIAS Center for Advanced Computation for providing computing resources.

## A Master Integrals

Reduction of Feynman integrals to master integrals is performed in the Euclidean space with  $d = 4 - 2\varepsilon$  dimensions. Our convention for the master integral with  $n$ -propagators  $(\mathcal{P}_1, \mathcal{P}_2, \dots, \mathcal{P}_n)$ , and  $h$ -loops is

$$(\mu e^{\gamma_E/2})^{h(4-d)} \int \prod_{j=1}^h \left( \frac{d^d l_j}{i\pi^{d/2}} \right) \frac{1}{\mathcal{P}_1 \mathcal{P}_2 \dots \mathcal{P}_n}, \quad (\text{A.1})$$

where  $l_j$  are loop momenta. In order to simplify the form of master integrals, several parameters are defined as follows,

$$\begin{aligned} x &= -\frac{q^2}{m_1^2} - i0, \quad r = \frac{m_2^2}{m_1^2}, \quad \tilde{r} = \frac{m_3^2}{m_1^2}, \\ y &= \frac{\sqrt{x+4} - \sqrt{x}}{\sqrt{x+4} + \sqrt{x}}, \\ \kappa_{1,2} &= \frac{1}{2} \pm \frac{\sqrt{x(x+4)}}{2x}, \\ \eta_{1,2} &= \frac{r+x-1}{2x} \pm \frac{1}{2x} \sqrt{r^2 + 2r(x-1) + (x+1)^2}, \\ \rho_{1,2} &= \frac{\tilde{r}-r+x}{2x} \pm \frac{1}{2x} \sqrt{r^2 - 2r(\tilde{r}-x) + (\tilde{r}+x)^2}, \end{aligned} \quad (\text{A.2})$$

where the subscript 1(2) is associated with a plus(minus) sign.

The master integrals shown in figure 19 are given in terms of the  $\varepsilon$ -expansion as follows,

$$I_1 = -m^2 \left( \frac{\mu^2}{m^2} \right)^\varepsilon (e^{\gamma_E \varepsilon}) \Gamma(-1 + \varepsilon), \quad (\text{A.3})$$

$$I_{21} = \left( \frac{\mu^2}{-q^2} \right)^\varepsilon (e^{\gamma_E \varepsilon}) \frac{\Gamma(1 - \varepsilon)^2 \Gamma(\varepsilon)}{\Gamma(2 - 2\varepsilon)}, \quad (\text{A.4})$$

$$\begin{aligned} I_{22} &= \left( \frac{\mu^2}{m_1^2} \right)^\varepsilon \left[ \frac{1}{\varepsilon} + (\eta_2 - 1) \ln(\eta_1 x + 1) + (\eta_1 - 1) \ln(\eta_2 x + 1) + 2 \right. \\ &\quad \left. + J_{22}^{(1)}(x, r) \varepsilon + \mathcal{O}(\varepsilon^2) \right], \end{aligned} \quad (\text{A.5})$$

$$I_{31} = m_1^2 \left( \frac{\mu^2}{m_1^2} \right)^{2\varepsilon} \left[ \frac{(1+r)}{2\varepsilon^2} + \left( \frac{3(1+r)}{2} - r \ln(r) \right) \frac{1}{\varepsilon} + (1-r) \text{Li}_2(1-r) \right. \\ \left. + \frac{1}{12} (42 + \pi^2) (r+1) + \frac{1}{2} r \ln^2(r) - 3r \ln(r) + \mathcal{O}(\varepsilon) \right], \quad (\text{A.6})$$

$$I_{32} = m_1^2 \left( \frac{\mu^2}{m_1^2} \right)^{2\varepsilon} \left[ \frac{1}{\varepsilon^2} + \frac{1}{\varepsilon} \left( 3 + \frac{x}{4} \right) + 6 + \frac{\pi^2}{6} + \frac{13}{8} x \right. \\ \left. + \left( \frac{x}{2} - 1 \right) \frac{1+y}{1-y} \ln y - \left( \frac{1+x}{x} \right) \ln^2 y + \mathcal{O}(\varepsilon) \right], \quad (\text{A.7})$$

$$I_{33} = \left( \frac{\mu^2}{m_1^2} \right)^{2\varepsilon} \left[ -\frac{1}{2\varepsilon^2} - \frac{1}{\varepsilon} \left( \frac{3}{2} + \frac{1+y}{1-y} \ln y \right) - \frac{9}{2} - \frac{\pi^2}{12} \right. \\ \left. + \frac{1+y}{1-y} \left( 6\text{Li}_2(-y) + 2\text{Li}_2(y) - 2\ln^2(y) \right) \right. \\ \left. + \left( 2\ln(1-y) + 6\ln(1+y) - 3 \right) \ln y + \frac{\pi^2}{6} \right) + \frac{(1+x)}{x} \ln^2 y + \mathcal{O}(\varepsilon) \right], \quad (\text{A.8})$$

$$I_{34} = \left( \frac{\mu^2}{m_1^2} \right)^{2\varepsilon} \left[ \frac{1}{2\varepsilon^2} + \frac{1}{2\varepsilon} - \frac{1}{2} + \frac{\pi^2}{12} - \frac{1+y}{1-y} \ln y - \left( \frac{1}{x} + \frac{1}{2} \right) \ln^2 y + \mathcal{O}(\varepsilon) \right], \quad (\text{A.9})$$

$$I_{35} = m_1^2 \left( \frac{\mu^2}{m_1^2} \right)^{2\varepsilon} \left[ \frac{1+r}{2\varepsilon^2} + \left( \frac{3(r+1)}{2} + \frac{x}{4} - r \ln(r) \right) \frac{1}{\varepsilon} + J_{35}(x, r) + J_{35}^{(1)}(x, r) \varepsilon + \mathcal{O}(\varepsilon^2) \right], \quad (\text{A.10})$$

$$I_{36} = \left( \frac{\mu^2}{m_1^2} \right)^{2\varepsilon} \left[ -\frac{1}{2\varepsilon^2} - \left( (\eta_2 - 1) \ln(\eta_1 x + 1) + (\eta_1 - 1) \ln(\eta_2 x + 1) + \frac{3}{2} \right) \frac{1}{\varepsilon} \right. \\ \left. + J_{36}(x, r) + \mathcal{O}(\varepsilon) \right], \quad (\text{A.11})$$

$$I_{37} = \left( \frac{\mu^2}{m_1^2} \right)^{2\varepsilon} \left[ \frac{1}{2\varepsilon^2} + \frac{1}{2\varepsilon} + J_{37}(x, r) + J_{37}^{(1)}(x, r) \varepsilon + \mathcal{O}(\varepsilon^2) \right], \quad (\text{A.12})$$

$$I_{4i} = \left( \frac{\mu^2}{m_1^2} \right)^{2\varepsilon} \left[ \frac{1}{2\varepsilon^2} + \left( (\eta_2 - 1) \ln(\eta_1 x + 1) + (\eta_1 - 1) \ln(\eta_2 x + 1) + \frac{5}{2} \right) \frac{1}{\varepsilon} \right. \\ \left. + J_{4i}(x, r, \tilde{r}) + \mathcal{O}(\varepsilon) \right], \quad (\text{A.13})$$

$$I_{5i} = \frac{1}{m_1^2} J_{5i}(x, r, \tilde{r}) + \mathcal{O}(\varepsilon). \quad (\text{A.14})$$

The results of the *multiple inverse binomial sums* in ref. [31] are used for  $I_{32}$ ,  $I_{33}$  and  $I_{34}$ .

The higher transcendental functions  $J_{ij}$  and  $J_{ij}^{(1)}$  are, respectively, the zeroth- and first-order terms in the  $\varepsilon$ -expansion of the master integrals. The functions with polylogarithms up to second order are given by,

$$J_{22}^{(1)}(x, r) = \frac{(-r+x+1)}{4x} \ln^2(r) + \frac{\pi^2}{12} + 4$$

$$\begin{aligned}
& + \left[ \left( 2(\eta_2 - 1) + \frac{1}{2}(\eta_1 - \eta_2) \ln \left( -(\eta_1 - \eta_2)^2 x^2 \right) \right) \ln(\eta_1 x + 1) \right. \\
& \quad \left. + (\eta_2 - \eta_1) \text{Li}_2 \left( \frac{1}{\eta_1} \right) + \frac{1}{2}(\eta_2 - \eta_1) \text{Li}_2 \left( \frac{\eta_2 x + 1}{\eta_1 x + 1} \right) + (\eta_1 \leftrightarrow \eta_2) \right], \quad (\text{A.15})
\end{aligned}$$

$$\begin{aligned}
J_{35}(x, r) &= \left( \frac{r}{2x} + r \right) \ln^2(r) + \left( 3 + \frac{\pi^2}{12} \right) (r + 1) + \frac{13x}{8} \\
& + \left[ \frac{1}{2}(\eta_2(-r + x - 1) - 6r - x + 1) \ln(\eta_1 x + 1) \right. \\
& \quad \left. - \frac{r(x + 1)}{2x} \ln^2(\eta_1 x + 1) + (1 - r) \text{Li}_2 \left( \frac{1}{\eta_1} \right) + (\eta_1 \leftrightarrow \eta_2) \right], \quad (\text{A.16})
\end{aligned}$$

$$\begin{aligned}
J_{36}(x, r) &= \left( \frac{r}{4x} - \frac{3(x + 1)}{4x} \right) \ln^2(r) - \frac{\pi^2}{12} - \frac{9}{2} \\
& + \left[ 3 \left( 1 - \eta_2 - \frac{1}{2}(\eta_1 - \eta_2) \ln \left( -(\eta_1 - \eta_2)^2 x^2 \right) \right) \ln(\eta_1 x + 1) \right. \\
& + \left( 1 - \eta_2 + \frac{r}{2x} \right) \ln^2(\eta_1 x + 1) + \left( 2 - 4\eta_2 + \frac{r - 1}{x} \right) \text{Li}_2 \left( \frac{1}{\eta_1} \right) \\
& \quad \left. + \left( \frac{3(r + x - 1)}{2x} - 3\eta_2 \right) \text{Li}_2 \left( \frac{\eta_2 x + 1}{\eta_1 x + 1} \right) + (\eta_1 \leftrightarrow \eta_2) \right], \quad (\text{A.17})
\end{aligned}$$

$$\begin{aligned}
J_{37}(x, r) &= \frac{r \ln^2(r)}{2x} + \frac{\pi^2}{12} - \frac{1}{2} + \left[ -\frac{r}{2x} \ln^2(\eta_1 x + 1) \right. \\
& \quad \left. + (1 - \eta_2) \ln(\eta_1 x + 1) + \text{Li}_2 \left( \frac{1}{\eta_1} \right) + (\eta_1 \leftrightarrow \eta_2) \right], \quad (\text{A.18})
\end{aligned}$$

$$\begin{aligned}
J_{41}(x, r) &= \frac{(1 - r)}{2x} \ln^2(r) - 4 \ln(r) + \frac{(1 - r)}{r} \text{Li}_2(1 - r) + \frac{19}{2} \\
& - \frac{1}{rx} \ln(-x) \ln(x + 1) + \pi^2 \left( \frac{1}{3rx} + \frac{1}{12} \right) \\
& + \left( 1 - 2\kappa_1 + \frac{2 \ln(-\kappa_1)}{rx} + \frac{\ln(-x)}{rx} \right) \ln(\kappa_1 x + 1) \\
& + \frac{(x - 1)}{rx} \ln^2(\kappa_1 x + 1) + \frac{(x + 1)}{rx} \left( \text{Li}_2 \left( \frac{1}{\kappa_1} \right) + \text{Li}_2 \left( \frac{1}{\kappa_2} \right) \right) \\
& - \frac{1}{rx} \left( \text{Li}_2 \left( \frac{x + 1}{\kappa_1 x + 1} \right) + \text{Li}_2 \left( \frac{x + 1}{\kappa_2 x + 1} \right) + \text{Li}_2(-x) \right) \\
& + \left[ \eta_1 \left( \frac{\pi^2}{6} + \ln((\eta_1 - \eta_2)x) \ln(\eta_1 x + 1) \right. \right. \\
& \quad \left. + \left( 4 + \ln(\eta_1 x + 1) - \ln((\eta_1 - \eta_2)x) \right) \ln(\eta_2 x + 1) \right. \\
& \quad \left. - \text{Li}_2 \left( \frac{1}{\eta_1} \right) + \text{Li}_2 \left( \frac{1}{\eta_2} \right) - \text{Li}_2 \left( \frac{\eta_2 x + 1}{\eta_1 x + 1} \right) \right]
\end{aligned}$$

$$\begin{aligned}
& + \frac{(r-1)\eta_1}{r} \left( -\ln(\eta_1(1-r)) \ln(\eta_2 x + 1) + \text{Li}_2\left(\frac{1}{\eta_1}\right) \right. \\
& + \text{Li}_2\left(\frac{\eta_1-1}{\eta_1-\kappa_1}\right) - \text{Li}_2\left(\frac{\eta_1}{\eta_1-\kappa_1}\right) + \text{Li}_2\left(\frac{\eta_1-1}{\eta_1-\kappa_2}\right) \\
& \left. - \text{Li}_2\left(\frac{\eta_1}{\eta_1-\kappa_2}\right) \right) + (\eta_1 \leftrightarrow \eta_2) \Bigg], \quad (\text{for } x > -1) \tag{A.19} \\
J_{42}(x, r, \tilde{r}) = & -\frac{(\tilde{r}-2)(1-r+x)}{2x} \ln^2(r) - \frac{1}{2} \tilde{r} \ln^2(\tilde{r}) - \rho_1 \ln(r) + (\rho_1-1) \ln(\tilde{r}) \\
& + (1-\tilde{r}) \text{Li}_2(1-\tilde{r}) + \frac{\pi^2}{12} + \frac{19}{2} + \ln\left(\frac{\rho_1 x}{r} + 1\right) \left( \frac{2r\tilde{r}}{x} \ln\left(\frac{r}{\tilde{r}}\right) - \rho_1 + \rho_2 \right) \\
& + \frac{2r\tilde{r}}{x} \ln^2\left(\frac{\rho_1 x}{r} + 1\right) - \frac{\tilde{r}(r+x)}{x} \left( \text{Li}_2\left(\frac{1}{1-\rho_1}\right) + \text{Li}_2\left(\frac{1}{1-\rho_2}\right) \right) \\
& + \frac{r\tilde{r}}{x} \left( \text{Li}_2\left(\frac{1-\rho_1}{\rho_1(\rho_2-1)}\right) + \text{Li}_2\left(\frac{1-\rho_2}{\rho_2(\rho_1-1)}\right) - \text{Li}_2\left(-\frac{x}{r}\right) \right) \\
& + \left[ (\eta_1-1) \left( \frac{\pi^2}{6} + \frac{\ln^2(r)}{2} + \ln((\eta_1-\eta_2)x) \ln(\eta_1 x + 1) \right. \right. \\
& - \ln^2(\eta_1 x + 1) + \left. \left( 4 - \ln(\tilde{r}) - \ln((\eta_1-\eta_2)x) \right) \ln(\eta_2 x + 1) \right. \\
& + \left. \text{Li}_2\left(\frac{1}{1-\eta_1}\right) - \text{Li}_2\left(\frac{1}{1-\eta_2}\right) - \text{Li}_2\left(\frac{\eta_2 x + 1}{\eta_1 x + 1}\right) \right) \\
& + (\eta_1-1)(\tilde{r}-1) \left( -\frac{1}{2} \ln^2(r) + \ln(\eta_2 x + 1) \ln\left(\frac{(1-\tilde{r})(\eta_1-1)}{\tilde{r}}\right) \right. \\
& + \left. \text{Li}_2\left(\frac{1}{1-\eta_1}\right) + \text{Li}_2\left(\frac{\eta_1}{\eta_1+\rho_1-1}\right) + \text{Li}_2\left(\frac{\eta_1}{\eta_1+\rho_2-1}\right) \right. \\
& \left. \left. - \text{Li}_2\left(\frac{\eta_1-1}{\eta_1+\rho_1-1}\right) - \text{Li}_2\left(\frac{\eta_1-1}{\eta_1+\rho_2-1}\right) \right) + (\eta_1 \leftrightarrow \eta_2) \right]. \tag{A.20} \\
& (\text{for } x > -r)
\end{aligned}$$

We stress that Eqs. (A.15), (A.16), (A.17) and (A.18) are valid for all values of  $x$  and  $r$ . The constraints on the allowed values of  $x$  and  $r$  in Eqs. (A.19) and (A.20) are valid for our calculation because  $m_1$ , the messenger fermion mass, is much larger than the gaugino mass. We check that Eq. (A.15) gives a consistent result of ref. [32]. The functions  $J_{35}(x, r)$  and  $J_{37}(x, r)$  are compatible with the result of ref. [33] which uses differential equation method.

The higher transcendental functions with polylogarithm up to third order are given by,

$$\begin{aligned}
J_{35}^{(1)}(x, r) = & \frac{5}{16} (12r + 23x + 12) + \frac{\pi^2}{24} (6r + x + 6 + 4 \ln(r)) - \frac{2\zeta(3)}{3} \left( \frac{r(9+5x)}{x} + 5 \right) \\
& + \ln^2(r) \left( \frac{24rx + r(r+12) + 3x^2 - 3}{8x} + \frac{3}{4} (r-1) \ln(-x) \right) - \frac{1}{3} \ln^3(r)
\end{aligned}$$



$$\begin{aligned}
& + \left[ -\ln(\eta_1 x + 1) \left( \frac{13}{4} \eta_2 (r - x + 1) + 6r + \frac{\pi^2}{6} (r + 1) + \frac{13}{4} (x - 1) \right. \right. \\
& \quad \left. \left. + \frac{3}{4} (\eta_1 - \eta_2) (r - x + 1) \ln(-(\eta_1 - \eta_2)^2 x^2) \right) \right. \\
& \quad + \ln^2(\eta_1 x + 1) \left( \frac{1}{2} \eta_2 (-r + x - 1) - \frac{3}{2} (r - 1) \ln(-x) \right. \\
& \quad \left. + \frac{r^2 - 6r(x + 1) - 2(x - 1)x}{4x} + \left( 1 - \frac{r(7x + 5)}{4x} \right) \ln(r) \right) \\
& \quad + \ln^3(\eta_1 x + 1) \left( \frac{r(3x + 1)}{2x} - \frac{4}{3} \right) + \text{Li}_2 \left( \frac{1}{\eta_1} \right) \left( \frac{r^2 - 1}{2x} - 3r - x + 5 \right. \\
& \quad \left. - 2\eta_2 (r - x + 1) + \left( \frac{r(2x - 1)}{x} - 3 \right) \ln(r) + \left( 2 - \frac{2r(2x + 1)}{x} \right) \ln(\eta_2 x + 1) \right) \\
& \quad + 3(r - 1) \text{Li}_2 \left( \frac{\eta_2}{\eta_1} \right) \left( \ln(\eta_2 x + 1) - \frac{\ln(r)}{2} \right) \\
& \quad + \text{Li}_2 \left( \frac{\eta_2 x + 1}{\eta_1 x + 1} \right) \left( \frac{3}{4} (\eta_1 - \eta_2) (r - x + 1) + \frac{3r(x + 1)}{x} \left( \frac{\ln(r)}{2} - \ln(\eta_2 x + 1) \right) \right) \\
& \quad + \text{Li}_3 \left( \frac{1}{\eta_1} \right) \left( \frac{2r(2x + 3)}{x} + 2 \right) + \text{Li}_3 \left( \frac{1}{1 - \eta_1} \right) \left( \frac{2r(x + 3)}{x} + 4 \right) \\
& \quad + \left( \text{Li}_3 \left( \frac{1 - \eta_2}{1 - \eta_1} \right) - \text{Li}_3 \left( \frac{\eta_2}{\eta_1} \right) \right) \frac{3}{2} (r - 1) \\
& \quad \left. + \frac{3}{2} \text{Li}_3 \left( \frac{\eta_2 x + 1}{\eta_1 x + 1} \right) \left( \frac{2r}{x} + r + 1 \right) + (\eta_1 \leftrightarrow \eta_2) \right], \tag{A.21}
\end{aligned}$$

$$\begin{aligned}
J_{37}^{(1)}(x, r) &= -\frac{11}{2} + \frac{\pi^2}{12} (2 \ln(r) + 1) - \zeta(3) \left( \frac{6r}{x} + \frac{10}{3} \right) \\
& - \ln^2(r) \left( \frac{3 - 5r + 3x}{4x} + \frac{3}{4} \ln(-x) \right) - \frac{1}{3} \ln^3(r) \\
& + \left[ \ln(\eta_1 x + 1) \left( 5(1 - \eta_2) - \frac{\pi^2}{6} - \frac{3}{2} (\eta_1 - \eta_2) \ln(-(\eta_1 - \eta_2)^2 x^2) \right) \right. \\
& \quad + \ln^2(\eta_1 x + 1) \left( 1 - \eta_2 - \frac{r}{2x} + \left( 1 - \frac{5r}{4x} \right) \ln(r) + \frac{3}{2} \ln(-x) \right) \\
& \quad + \ln^3(\eta_1 x + 1) \left( \frac{r}{2x} - \frac{4}{3} \right) + \frac{3}{2} \text{Li}_2 \left( \frac{\eta_2}{\eta_1} \right) \left( \ln(r) - 2 \ln(\eta_2 x + 1) \right) \\
& \quad \left. + \text{Li}_2 \left( \frac{1}{\eta_1} \right) \left( 4(1 - \eta_2) + \frac{r - 1}{x} - \left( \frac{r}{x} + 3 \right) \ln(r) + \left( 2 - \frac{2r}{x} \right) \ln(\eta_2 x + 1) \right) \right]
\end{aligned}$$

$$\begin{aligned}
& + \frac{3}{2} \text{Li}_2 \left( \frac{\eta_2 x + 1}{\eta_1 x + 1} \right) \left( \eta_1 - \eta_2 + \frac{r}{x} \left( \ln(r) - 2 \ln(\eta_2 x + 1) \right) \right) \\
& + \text{Li}_3 \left( \frac{1}{\eta_1} \right) \left( \frac{6r}{x} + 2 \right) + \text{Li}_3 \left( \frac{1}{1 - \eta_1} \right) \left( \frac{6r}{x} + 4 \right) + \frac{3}{2} \text{Li}_3 \left( \frac{\eta_2}{\eta_1} \right) \\
& - \frac{3}{2} \text{Li}_3 \left( \frac{1 - \eta_2}{1 - \eta_1} \right) + \text{Li}_3 \left( \frac{\eta_2 x + 1}{\eta_1 x + 1} \right) \left( \frac{3r}{x} + \frac{3}{2} \right) + (\eta_1 \leftrightarrow \eta_2) \Big]. \tag{A.22}
\end{aligned}$$

As for  $J_{5i}$  ( $i = 1, 2, 3, 4$ ) we need transcendental functions higher than polylogarithm of order 3. Their analytic expressions are beyond the scope of this paper. Instead they can be given by a definite integral so that numerical evaluation of them is easily performed. To this end, we use the differential equation method in ref. [34]. For example, differentiating  $I_{51}$  by  $m_2^2$  is represented by a linear combination of other master integrals in a diagrammatic way. By solving the differential equation, one can express the function  $J_{51}$  as a definite

integral.

After all, the functions  $J_{5i}$  ( $i = 1, 2, 3, 4$ ) are given by definite integrals of functions as follows,

$$J_{5i}(x, r) = \int_1^r dr' f_i(x, r') \left[ \sum_{j \geq 1} c_{ij}(x, r') \mathcal{J}_{ij}(x, r') + c_{i0}(x, r') \right] - \frac{\hat{J}_i(x)}{x}, \tag{A.23}$$

$$\begin{aligned}
J_{54}(x, r, \tilde{r}) &= \int_1^r dr' f_4(x, r', \tilde{r}) \left[ \sum_{j \geq 1} c_{4j}(x, r', \tilde{r}) \mathcal{J}_{4j}(x, r', \tilde{r}) + c_{40}(x, r', \tilde{r}) \right] \\
&+ \int_1^{\tilde{r}} dr' \tilde{f}_4(x, r') \left[ \sum_{j \geq 1} \tilde{c}_{4j}(x, r') \tilde{\mathcal{J}}_{4j}(x, r') + \tilde{c}_{40}(x, r') \right] - \frac{\hat{J}_4(x)}{x}, \tag{A.24}
\end{aligned}$$

where  $\mathcal{J}_{ij}$  are a set of known master integral functions, and  $\hat{J}_i(x)$ 's are the master integral functions in the limit that all the masses are equal. One can find the expressions for  $\hat{J}_i(x)$  in ref. [35, 36]:

$$\hat{J}_1(x) = 2 \ln^2(y) \ln(1 - y) + 6\zeta(3) - 6\text{Li}_3(y) + 6 \ln(y) \text{Li}_2(y), \tag{A.25}$$

$$\begin{aligned}
\hat{J}_{2,3,4}(x) &= 6\zeta(3) + 12\text{Li}_3(y) + 24\text{Li}_3(-y) - 8 \ln(y) (\text{Li}_2(y) + 2\text{Li}_2(-y)) \\
&- 2 \ln^2(y) (\ln(1 - y) + 2 \ln(1 + y)). \tag{A.26}
\end{aligned}$$

The coefficient functions  $c_{ij}(x, r)$ , the factor functions  $f_i(x, r)$  and the corresponding set of master integrals  $\mathcal{J}_{ij}(x, r)$  are given by,

$$f_1(x, r) = r^{-1} x^{-3} (\eta_1 - \eta_2)^{-2},$$

$$\begin{aligned}
\mathcal{J}_{1j}(x, r) &= \left\{ J_{22}^{(1)}(x, r), J_{35}(x, r), J_{37}(x, r), J_{37}\left(\frac{x}{r}, \frac{1}{r}\right), J_{41}\left(\frac{x}{r}, \frac{1}{r}\right) \right\}, \\
c_{11}(x, r) &= -c_{15}(x, r) = \frac{x(x+4)}{r-1} + 3x, \\
c_{12}(x, r) &= -2(r+x+1), \\
c_{13}(x, r) &= \frac{x(x+4)}{r-1} + 4x + r + 1, \\
c_{14}(x, r) &= -\frac{rx(x+4)}{r-1} + r(r+1), \\
c_{10}(x, r) &= (1-r)(r+x+1)\text{Li}_2(1-r) + \frac{\pi^2}{12}(r+x+1)^2 + \frac{11x(x+4)}{2(r-1)} \\
&\quad + \frac{1}{4}\left(37rx + 26(r+1)^2 + 11x^2 + 103x\right) \\
&\quad + \ln(r)\left(\frac{(1+2\eta_1)x(x+4)}{r-1} + \ln(x)\left(\eta_1 x(r+x+1) + \frac{x(x+4)}{r-1} + 3x\right) \right. \\
&\quad \left. - (7r-2)x - 6r(r+1) - x^2 + 6\eta_1 x\right) \\
&\quad + \ln^2(r)\left(\frac{(\eta_1-1)x(x+4)}{r-1} - \eta_1 x(r+x-2) + \frac{3}{2}r(r+x+1) - 3x\right) \\
&\quad + \frac{(1+y')}{(1-y')}\ln(y')\left(\frac{x(x+4)}{r-1} + 3x\right) + \ln^2(y')\left(\frac{(x+2)(x+4)}{2(r-1)} \right. \\
&\quad \left. + 2r^2 + \frac{5r(x+2)}{2} + \frac{(x+2)(x+4)}{2}\right) \\
&\quad - (\eta_1 - \eta_2)\ln(\eta_1 x + 1)\left(\frac{2x(x+4)}{r-1} + x(r+x+1)\ln(x) + 6x \right. \\
&\quad \left. + \ln(r)\left(\frac{x(x+4)}{r-1} - x(r+x-2)\right)\right), \tag{A.27}
\end{aligned}$$

$$\begin{aligned}
f_2(x, r) &= r^{-1}x^{-4}(\eta_1 - \eta_2)^{-4}, \\
\mathcal{J}_{2j}(x, r) &= \left\{ J_{22}^{(1)}(x, r), J_{35}(x, r), J_{37}(x, r), J_{37}\left(\frac{x}{r}, \frac{1}{r}\right), J_{35}^{(1)}(x, r), J_{37}^{(1)}(x, r), J_{37}^{(1)}\left(\frac{x}{r}, \frac{1}{r}\right) \right\}, \\
c_{21}(x, r) &= (\eta_1 - \eta_2)^2 x^2 (r - x - 1), \\
c_{22}(x, r) &= 15r^2 + 8r(x-1) - 7(x+1)^2, \\
c_{23}(x, r) &= -4(r^2 + 4rx - (x+1)^2), \\
c_{24}(x, r) &= (-r+x+1)\left(9r^2 + 2r(5x-1) + (x+1)^2\right) - 4r(r-x-1)(r+x)\ln(r), \\
c_{25}(x, r) &= 2(-r+x+1)(r+x+1), \\
c_{26}(x, r) &= 2(x+1)(r-x-1), \\
c_{27}(x, r) &= 2r(r-x-1)(r+x), \\
c_{20}(x, r) &= \frac{4}{3}\zeta(3)r(-r+x+1) - \frac{\pi^2}{12}\left(3r^3 + r^2(7x+3) + r(x+1)(5x-7) + (x+1)^3\right)
\end{aligned}$$

$$\begin{aligned}
& -35r^3 - r^2 \left( \frac{77}{2}x + 9 \right) - r(x-5)(2x+7) + \frac{3}{2}(x+1)^2(x+6) \\
& + \ln(r) \left( 33r^3 - r^2(25-27x) - \frac{1}{3}\pi^2 r(r-x-1) \right. \\
& \quad \left. - r(x+1)(5x+9) + (x+1)^3 \right) + \ln^2(r) \left( \eta_1 (\eta_1 - \eta_2)^2 x^2 (r+x+1) \right. \\
& \quad \left. - \frac{1}{2} (19r^3 + 3r^2(5x-7) - r(x+1)(3x-1) + (x+1)^3) \right) \\
& - \frac{1}{3} \ln^3(r) r(r-x-1)(4r+4x+1) \\
& + (\eta_1 - \eta_2)^2 \ln(\eta_1 x + 1) \ln(r) \left( x(-r+x+1)(r+x-1) - 2\eta_1 x^2(r+x+1) \right) \\
& + 2(\eta_1 - \eta_2)^2 \ln^2(\eta_1 x + 1) r x(r+x-1), \tag{A.28}
\end{aligned}$$

$$f_3(x, r) = (2r+x+2)^{-1} x^{-2} (\eta_1 - \eta_2)^{-2},$$

$$\mathcal{J}_{3j}(x, r) = \left\{ J_{22}^{(1)}(x, r), J_{41}(x, r), J_{41}\left(\frac{x}{r}, \frac{1}{r}\right) \right\},$$

$$c_{31}(x, r) = -\frac{2x(x+4)}{r-1} - 2x,$$

$$c_{32}(x, r) = \frac{2x(x+4)}{r-1} + 2x - 4,$$

$$c_{33}(x, r) = 4,$$

$$\begin{aligned}
c_{30}(x, r) = & -4\text{Li}_2(1-r)(r+x+3) - \frac{11x(r+x+3)}{r-1} - \ln(r) \left( \frac{4(\eta_1-1)x(r+x+3)}{r-1} + 16 \right) \\
& - \ln^2(r) \left( 2\eta_1(r+x+5) + \frac{(x+4)^2}{r-1} + 2r+3x+8 \right) \\
& + \ln(\eta_1 x + 1) \left( \ln(r) \left( \frac{2(r(x-2)+x^2+x+2)}{x} + 4\eta_1(r+x+5) \right. \right. \\
& \quad \left. \left. + \frac{2(x+4)(r+x+3)}{r-1} \right) + \frac{4(\eta_1 - \eta_2)x(r+x+3)}{r-1} \right) \\
& - 2\ln^2(\eta_1 x + 1) \frac{(\eta_1 - \eta_2)^2 x(r+x+3)}{r-1} - 2\frac{(1+y)}{1-y} \ln(y) \left( \frac{x(x+4)}{r-1} + x-2 \right) \\
& - 4\frac{(1+y')}{1-y'} \ln(y') + \ln^2(y) \left( \frac{2(x+4)}{r-1} + \frac{4}{x} + 4 \right) \\
& + \ln^2(y') \left( \frac{4r(x-1)}{x} + \frac{(x+4)(2r+x+2)}{r-1} + 3(x+2) \right), \tag{A.29}
\end{aligned}$$

$$f_4(x, r, \tilde{r}) = \left( x(r-1)(\tilde{r}-1) + (r+\tilde{r}-2)(r\tilde{r}-1) \right)^{-1} x^{-2} (\eta_1 - \eta_2)^{-2},$$

$$\begin{aligned}
\mathcal{J}_{4j}(x, r, \tilde{r}) = & \left\{ J_{22}^{(1)}(x, r), J_{22}^{(1)}(x, \tilde{r}), J_{35}\left(\frac{x}{r}, \frac{\tilde{r}}{r}\right), J_{37}\left(\frac{x}{r}, \frac{\tilde{r}}{r}\right), J_{37}\left(\frac{x}{\tilde{r}}, \frac{r}{\tilde{r}}\right), J_{41}(x, r), J_{41}(x, \tilde{r}), \right. \\
& \left. J_{42}(x, r, \tilde{r}), J_{42}(x, \tilde{r}, r) \right\},
\end{aligned}$$

$$\begin{aligned}
c_{41}(x, r, \tilde{r}) &= r^2 \tilde{r} + \frac{x(x+4)(\tilde{r}-1)}{r-1} + r(x\tilde{r} - \tilde{r} - x - 1) + x(3\tilde{r} + x + 1) + 1, \\
c_{42}(x, r, \tilde{r}) &= -x^2(\eta_1 - \eta_2)^2 \left( \frac{\tilde{r}-1}{r-1} + \tilde{r} \right), \\
c_{43}(x, r, \tilde{r}) &= 2r \left( x(1 - \tilde{r}) - r\tilde{r} - r - \tilde{r} + 3 \right), \\
c_{44}(x, r, \tilde{r}) &= \frac{x(x+4)(\tilde{r}-1)}{r-1} + x(2r\tilde{r} - 3r + 2\tilde{r}) + r(2r\tilde{r} + r + \tilde{r} - 5) - \tilde{r} - x + 2, \\
c_{45}(x, r, \tilde{r}) &= \tilde{r} \left( r(\tilde{r} - 2x + 3) + (x+1)\tilde{r} - r^2 - x(x+3) - 4 \right), \\
c_{46}(x, r, \tilde{r}) &= -\frac{x(x+4)(\tilde{r}-1)}{r-1} - x(r\tilde{r} - 2r + 2\tilde{r} - 1) - (r-1)(r\tilde{r} + \tilde{r} - 2), \\
c_{47}(x, r, \tilde{r}) &= x^2(\eta_1 - \eta_2)^2 \tilde{r}, \\
c_{48}(x, r, \tilde{r}) &= -x^2 - x(r + \tilde{r} + 2) + r\tilde{r} - r - \tilde{r} + 1, \\
c_{49}(x, r, \tilde{r}) &= x^2(\eta_1 - \eta_2)^2 \frac{\tilde{r}-1}{r-1}, \\
c_{40}(x, r, \tilde{r}) &= (r-1)\text{Li}_2(1-r)(3+x-r-\tilde{r}(r+x+1)) \\
&\quad + \text{Li}_2(1-\tilde{r})(r-x-3-\tilde{r}^2(r+x+1)+2\tilde{r}(x+2)) \\
&\quad + \frac{1}{4}(26r^2 - r(39x+82) + x(9x+25) + 4) + \frac{x(x+4)(\tilde{r}-1)}{2(r-1)} \\
&\quad + \frac{\tilde{r}}{4}(26r^2 + r(15x+56) - x(11x+35) - 82) + \frac{13}{2}\tilde{r}^2(r+x+1) \\
&\quad + \frac{\pi^2}{12} \left( \tilde{r}^2(r+x+1) + \tilde{r}((r+x)^2 - x - 1) - \frac{x(x+4)(\tilde{r}-1)}{r-1} \right. \\
&\quad \left. + (r+1)(r+x-2) \right) + \ln(r) \left( \tilde{r}(r^2 + 2r(x+3) + (x-3)x - 19) \right. \\
&\quad \left. + 6\tilde{r}^2(r+x+1) + \frac{x(x+4)(\tilde{r}-1)}{r-1} - r(x+2) - x(x+4) + 2 \right) \\
&\quad - \ln(\tilde{r}) \left( \tilde{r}(r^2 + 2r(x+2) + (x-4)x - 17) + 6\tilde{r}^2(r+x+1) \right) \\
&\quad + \ln^2(r) \left( 2\tilde{r}^2(r+x+1) + \frac{1}{2}\tilde{r}(3r-2x-13) + \frac{x(x+4)(\tilde{r}-1)}{2(r-1)} \right. \\
&\quad \left. - \frac{1}{2}(r+1)(r+x-2) \right) + \ln^2(\tilde{r}) \left( \frac{1}{2}\tilde{r}(-r^2 + r(5-2x) - x(x+5) - 10) \right. \\
&\quad \left. + \frac{3}{2}\tilde{r}^2(r+x+1) \right) + 4\ln(r)\ln(\tilde{r})(\tilde{r}(-r+x+3) - \tilde{r}^2(r+x+1)) \\
&\quad + \frac{1+y}{1-y}\ln y \left( \tilde{r}(-r(x-2) - x^2 - 2) + \frac{x(x+4)(\tilde{r}-1)}{r-1} - 2r(x+1) - x + 2 \right) \\
&\quad + \ln^2 y \left( \tilde{r} \left( \frac{2(r-1)}{x} + 2r + \frac{3x}{2} + 1 \right) + \frac{(x+2)(x+4)(\tilde{r}-1)}{2(r-1)} \right. \\
&\quad \left. - \frac{r}{2x}(x^2 + 2x + 4) - \frac{(x+2)(x+6)}{2} + \frac{2}{x} \right)
\end{aligned}$$

$$\begin{aligned}
& + \left( (\eta_1 - 1) \ln(\eta_2 x + 1) + (\eta_2 - 1) \ln(\eta_1 x + 1) \right) \left( (\tilde{\eta}_1 - 1) \ln(\tilde{\eta}_2 x + 1) \right. \\
& \quad \left. + (\tilde{\eta}_2 - 1) \ln(\tilde{\eta}_1 x + 1) \right) \left( x(-r + x + 3) - x\tilde{r}(r + x + 1) \right) \\
& + \left( (\eta_1 - 1) \ln(\eta_2 x + 1) + (\eta_2 - 1) \ln(\eta_1 x + 1) \right) \left( -(\eta_1 - \eta_2)^2 x^2 \tilde{r} \ln(\tilde{r}) \right. \\
& \quad \left. + \frac{2x(x+4)(\tilde{r}-1)}{r-1} + \tilde{r}(2r(r+x-1) + 6x) + 2(-r(x+1) + x^2 + x + 1) \right) \\
& + \left( (\tilde{\eta}_1 - 1) \ln(\tilde{\eta}_2 x + 1) + (\tilde{\eta}_2 - 1) \ln(\tilde{\eta}_1 x + 1) \right) \\
& \quad \times \left( \ln(r) \left( \tilde{r}(r^2 + (r+2)x - 1) + \frac{x(x+4)(\tilde{r}-1)}{r-1} - 2r(x+1) - x + 2 \right) \right. \\
& \quad \left. - 2x^2 (\eta_1 - \eta_2)^2 \left( \frac{\tilde{r}-1}{r-1} + \tilde{r} \right) \right), \tag{A.30}
\end{aligned}$$

$$\begin{aligned}
\tilde{f}_4(x, r) &= (r-1)^{-1} x^{-2} (\eta_1 - \eta_2)^{-2}, \\
\tilde{\mathcal{J}}_{4j}(x, r) &= \left\{ J_{22}^{(1)}(x, r), J_{35}(x, r), J_{37}(x, r), J_{37}\left(\frac{x}{r}, \frac{1}{r}\right), J_{41}(x, r) \right\}, \\
\tilde{c}_{41}(x, r) &= -\tilde{c}_{45}(x, r) = r - x - 1, \\
\tilde{c}_{42}(x, r) &= -4, \\
\tilde{c}_{43}(x, r) &= -r - x + 3, \\
\tilde{c}_{44}(x, r) &= 3r - x - 1, \\
\tilde{c}_{40}(x, r) &= 2(1-r) \text{Li}_2(1-r) + \frac{\pi^2}{6}(r+x+1) + \frac{37r}{2} + \frac{15}{2} - \ln(r)(11r+x+1) \\
& + \frac{1}{2} \ln^2(r)(7r-x-1) + \frac{1+y}{1-y} \ln(y)(r-x-1)(\ln(r)+1) \\
& + \ln^2(y) \left( \frac{r-1}{x} + \frac{r+x+5}{2} \right) + \left( (\eta_1 - 1) \ln(\eta_2 x + 1) + (\eta_2 - 1) \ln(\eta_1 x + 1) \right) \\
& \quad \times \left( 2(r-x-1) - 2x \frac{(1+y)}{1-y} \ln(y) \right), \tag{A.31}
\end{aligned}$$

where the new variables are defined by

$$y' \equiv y|_{x \rightarrow x/r}, \quad \tilde{\eta}_1 \equiv \eta_1|_{r \rightarrow \tilde{r}}, \quad \tilde{\eta}_2 \equiv \eta_2|_{r \rightarrow \tilde{r}}. \tag{A.32}$$

For the calculation of the gluino pole mass, setting  $x \rightarrow 0$  leads to a good approximation of the self-energy function  $\Omega^{(2)}$ . In that limit, we can do the above integrations so that the analytic expressions of  $J_{5i}$  are given as follows:

$$\begin{aligned}
J_{51}(0, r) &= -\frac{(r+1)}{(r-1)^2} \text{Li}_2(1-r) - \frac{4}{r-1} + \frac{(3-r)}{(r-1)^2} \ln(r) - \frac{\ln^2(r)}{2(r-1)} \\
& \quad + \ln(x) \left( \frac{1}{r-1} - \frac{\ln(r)}{(r-1)^2} \right), \tag{A.33}
\end{aligned}$$

$$J_{52}(0, r) = J_{53}(0, r) = \frac{2}{r-1} \text{Li}_2(1-r) + \frac{r}{(r-1)^2} \ln^2(r), \tag{A.34}$$

$$\begin{aligned}
J_{54}(0, r, \tilde{r}) = & \frac{\text{Li}_2(1-r)}{\tilde{r}-1} + \frac{\text{Li}_2(1-\tilde{r})}{r-1} + \frac{\text{Li}_2(\tilde{r})}{\tilde{r}-1} \\
& - \frac{\pi^2}{6(r-1)} + \frac{r \ln(r) \ln(\tilde{r})}{(r-1)(\tilde{r}-1)} + \frac{\ln(1-\tilde{r}) \ln(\tilde{r})}{\tilde{r}-1} \\
& - \frac{(r-\tilde{r})}{(r-1)(\tilde{r}-1)} \left( \text{Li}_2\left(\frac{\tilde{r}}{r}\right) + \ln\left(\frac{\tilde{r}}{r}\right) \ln(r-\tilde{r}) + \frac{\ln^2(r)}{2} \right). \quad (\text{A.35})
\end{aligned}$$

It should be noted that there remains a singularity of  $\ln(x)$  in  $J_{51}(x, r)$  as  $x \rightarrow 0$ . We comment that the singularity can be handled using the asymptotic expansion technique [37, 38].

## B Explicit formula for $\Omega^{(2)}(s)$

Using the master integrals in Appendix A, we can write down the full expression of the self-energy function  $\Omega^{(2)}$  as follows,

$$\begin{aligned}
\Omega^{(2)}(s) = & \left( \frac{\alpha_s}{4\pi} \right)^2 \Lambda(r-1)^{-1} N_{\text{mess}} C(R) C_2(R) \left[ \right. \\
& - 4J_{22}^{(1)}(x, r) \left( \frac{r-x+1}{r} + \frac{((x+1)^2 + r(x-5))}{(\eta_1 - \eta_2)^2 r x} \right) \\
& + 4J_{35} \left( \frac{x}{r}, \frac{\tilde{r}}{r} \right) \left( r-x+2 + \frac{(x-2)(x+1)^2 + r(x^2 - 9x + 2)}{(\eta_1 - \eta_2)^2 x^2} \right) \\
& + 8J_{36}(x, r) + 4J_{37}(x, r) + 4J_{37} \left( \frac{x}{r}, \frac{1}{r} \right) \\
& - 2J_{37} \left( \frac{x}{r}, \frac{\tilde{r}}{r} \right) \left( 2r-3x+4 + \frac{2((x-1)(x+1)^2 + r(x^2 - 7x + 1))}{(\eta_1 - \eta_2)^2 x^2} \right) \\
& + 2J_{37} \left( \frac{x}{\tilde{r}}, \frac{r}{\tilde{r}} \right) \frac{(x^3 + 2x^2 + 3x + r(x^2 - 7x - 2) + 2)}{(\eta_1 - \eta_2)^2 x^2} \\
& + 4J_{41}(x, r) \left( \frac{r-x+1}{r} + \frac{(x+1)^2 + r(x-5)}{(\eta_1 - \eta_2)^2 r x} \right) \\
& + 2J_{41} \left( \frac{x}{r}, \frac{1}{r} \right) \left( r+3 - \frac{3r+x+1}{(\eta_1 - \eta_2)^2 x} \right) + 2J_{42}(x, r, \tilde{r}) \left( 1-r + \frac{3r+x+1}{(\eta_1 - \eta_2)^2 x} \right) \\
& - 4(r+x+1)J_{52}(x, r) + 2(r-1)(J_{54}(x, r, \tilde{r}) - J_{53}(x, r)) \\
& + \frac{2\text{Li}_2(1-r)}{r} \left( 2(r+4)x+3 + \frac{x^3 + (r-4)x^2 - (17r+13)x - 8}{(\eta_1 - \eta_2)^2 x} - (\eta_1 - \eta_2)^2 x^2 \right) \\
& - 2\text{Li}_2(1-\tilde{r}) \left( r + \frac{x^2 + (r+1)x - 8r}{(\eta_1 - \eta_2)^2 x} \right) + \frac{\pi^2}{6} \left( 2r + \frac{(x+1)(x^2 + 3x + r(x-4) + 4)}{(\eta_1 - \eta_2)^2 x^2} \right) \\
& - \frac{2(\eta_1 - \eta_2)^2 x^2}{r} + \frac{15x^2 + 88x - 144}{2r} \\
& - \frac{(11x^2 + 80x - 104)(x+1)^2 + r(11x^3 + 7x^2 - 680x + 104)}{2(\eta_1 - \eta_2)^2 r x^2} \\
& + 2\ln(r) \left( 2r-12x-19 + \frac{r(6x^2 - 23x - 12) + 3(2x^3 + 7x^2 + 9x + 4)}{(\eta_1 - \eta_2)^2 x^2} \right) \\
& \left. \right]
\end{aligned}$$

$$\begin{aligned}
& -12 \ln(\tilde{r}) \left( \frac{7r}{6} + \frac{x^3 + 2x^2 + 3x + r(x^2 - 7x - 2) + 2}{(\eta_1 - \eta_2)^2 x^2} \right) \\
& -2 \ln(r) \ln(\tilde{r}) \left( 4r + \frac{4x^3 + 7x^2 + 12x + r(4x^2 - 31x - 9) + 9}{(\eta_1 - \eta_2)^2 x^2} \right) \\
& + \ln^2(r) \left( 2(r+1) + \frac{3x(x^2 - 1) + r(3x^2 - 27x + 16)}{(\eta_1 - \eta_2)^2 x^2} \right) \\
& + \ln^2(\tilde{r}) \left( 2r + \frac{3(x^3 + 2x^2 + 3x + r(x^2 - 7x - 2) + 2)}{(\eta_1 - \eta_2)^2 x^2} \right) \\
& + \frac{4(1+y)}{1-y} \ln(y) \left( \frac{x-2}{r} - \frac{(x+1)^2 + r(x-5)}{(\eta_1 - \eta_2)^2 r x} \right) \\
& + \frac{1+y'}{1-y'} \ln(y') \left( \frac{2(3r+x+1)}{(\eta_1 - \eta_2)^2 x} - 4r \right) \\
& + \ln^2(y) \left( \frac{2(3x^2 + 5rx + 9x + 2r + 6)}{(\eta_1 - \eta_2)^2 r x^2} - \frac{8(x+1)}{r x} \right) + \ln^2(y') \left( x + \frac{4}{x} + 22 \right. \\
& \left. + r \left( 10 - \frac{8}{x} \right) + \frac{(3x-14)(x+1)^2 + r(3x^2 - 41x + 22)}{x^2 (\eta_1 - \eta_2)^2} - 4x (\eta_1 - \eta_2)^2 \right) \\
& + 4 \left( (\eta_1 - 1) \ln(\eta_2 x + 1) + (\eta_2 - 1) \ln(\eta_1 x + 1) \right)^2 \\
& - \left( (\eta_1 - 1) \ln(\eta_2 x + 1) + (\eta_2 - 1) \ln(\eta_1 x + 1) \right) \left( \frac{4(11r - 4x + 1)}{r} \right. \\
& \left. + \frac{16((x+1)^2 + r(x-3))}{(\eta_1 - \eta_2)^2 r x} + \ln(r) \left( 2r + \frac{4(x^2 + 3x - 2r + 2)}{(\eta_1 - \eta_2)^2 x^2} \right) \right. \\
& \left. - \ln(\tilde{r}) \left( \frac{4(r-2)}{(\eta_1 - \eta_2)^2 x} - 2r + 4 \right) \right) + 4 \ln \left( \frac{\mu^2}{M_{\text{mess}}^2} \right) \left( \ln(r) \left( \frac{r+x+1}{(\eta_1 - \eta_2)^2 x} - 1 \right) \right. \\
& \left. + \left( (\eta_1 - 1) \ln(\eta_2 x + 1) + (\eta_2 - 1) \ln(\eta_1 x + 1) \right) \left( \frac{r+x-1}{(\eta_1 - \eta_2)^2 x} - 2 \right) \right) \\
& \left. - (r \leftrightarrow \tilde{r}) \right] \\
& + \left( \frac{\alpha_s}{4\pi} \right)^2 \Lambda(r-1)^{-1} N_{\text{mess}} C(R) C_2(G) \left[ \right. \\
& - 3J_{22}^{(1)}(x, r) - \frac{16}{x} J_{35}(x, r) + J_{37}(x, r) \left( 2 + \frac{8}{x} - \frac{8}{r-1} \right) \\
& + J_{37} \left( \frac{x}{r}, \frac{1}{r} \right) \left( \frac{8x(\eta_1 - \eta_2)^2}{r-1} - \frac{8x^2 + 9rx + 15x - 8r + 8}{(r-1)x} \right) \\
& + 2J_{41}(x, r) + J_{42}(x, r, \tilde{r}) + J_{51}(x, r)(2 - 2r + x) + 4J_{51} \left( \frac{x}{r}, \frac{1}{r} \right) \left( 1 - \frac{1}{r} \right) \\
& \left. + 2J_{52}(x, r)(r + x + 1) + (r-1)(J_{53}(x, r) - J_{54}(x, r, \tilde{r})) + 8\text{Li}_2(1-r) \left( \frac{1-r}{x} \right) \right]
\end{aligned}$$



$$\begin{aligned}
& + \frac{2\pi^2 r}{3x} + \frac{52r}{x} + \ln(r) \left( 97 - \frac{48}{x} + \frac{48x+200}{r-1} - \frac{48(\eta_1 - \eta_2)^2 x}{r-1} - \ln(x) \left( \frac{6r+2}{r-1} \right) \right) \\
& + \frac{\ln^2(r)}{r-1} \left( 12x(\eta_1 - \eta_2)^2 - \frac{24x^2 + 43rx + 45x - 24r + 24}{2x} \right) \\
& + \frac{6(1+y')}{1-y'} \ln(y') + \ln^2(y') \left( 1 - \frac{2r}{x} \right) \\
& - 2 \left( (\eta_1 - 1) \ln(\eta_2 x + 1) + (\eta_2 - 1) \ln(\eta_1 x + 1) \right)^2 \\
& - \left( (\eta_1 - 1) \ln(\eta_2 x + 1) + (\eta_2 - 1) \ln(\eta_1 x + 1) \right) \left( 22 + \ln(r) - 6 \ln(x) \right) \\
& + 8 \ln \left( \frac{\mu^2}{M_{\text{mess}}^2} \right) - (r \leftrightarrow \tilde{r}) \Bigg]. \tag{B.1}
\end{aligned}$$

## References

- [1] M. Dine, W. Fischler and M. Srednicki, Phys. Lett. B **104** (1981) 199.
- [2] S. Dimopoulos and S. Raby, Nucl. Phys. B **192** (1981) 353.
- [3] M. Dine and W. Fischler, Phys. Lett. B **110**, 227 (1982).
- [4] C. R. Nappi and B. A. Ovrut, Phys. Lett. B **113**, 175 (1982).
- [5] L. Alvarez-Gaume, M. Claudson and M. B. Wise, Nucl. Phys. B **207**, 96 (1982).
- [6] S. Dimopoulos and S. Raby, Nucl. Phys. B **219**, 479 (1983).
- [7] M. Dine and A. E. Nelson, Phys. Rev. D **48** (1993) 1277 [arXiv:hep-ph/9303230].
- [8] M. Dine, A. E. Nelson and Y. Shirman, Phys. Rev. D **51** (1995) 1362 [arXiv:hep-ph/9408384].
- [9] M. Dine, A. E. Nelson, Y. Nir and Y. Shirman, Phys. Rev. D **53** (1996) 2658 [arXiv:hep-ph/9507378].
- [10] S. P. Martin, Phys. Rev. D **71** (2005) 116004 [hep-ph/0502168].
- [11] Y. Yamada, Phys. Lett. **B623** (2005) 104-110. [hep-ph/0506262].
- [12] S. P. Martin, Phys. Rev. **D72** (2005) 096008. [hep-ph/0509115].
- [13] R. Schofbeck and H. Eberl, Phys. Lett. B **649** (2007) 67 [hep-ph/0612276].
- [14] R. Schofbeck and H. Eberl, Eur. Phys. J. C **53** (2008) 621 [arXiv:0706.0781 [hep-ph]].
- [15] M. Picariello and A. Strumia, Nucl. Phys. B **529** (1998) 81 [hep-ph/9802446].
- [16] W. Siegel, Phys. Lett. **B84** (1979) 193.
- [17] D. M. Capper, D. R. T. Jones, P. van Nieuwenhuizen, Nucl. Phys. **B167** (1980) 479.
- [18] I. Jack, D. R. T. Jones, K. L. Roberts, Z. Phys. **C62** (1994) 161-166. [hep-ph/9310301].
- [19] H. K. Dreiner, H. E. Haber, S. P. Martin, Phys. Rept. **494** (2010) 1-196. [arXiv:0812.1594 [hep-ph]].
- [20] S. P. Martin, Phys. Rev. D **55** (1997) 3177 [hep-ph/9608224].

- [21] S. Dimopoulos, G. F. Giudice and A. Pomarol, Phys. Lett. B **389** (1996) 37 [hep-ph/9607225].
- [22] S. Laporta, Int. J. Mod. Phys. A **15**, 5087 (2000) [arXiv:hep-ph/0102033].
- [23] G. Passarino and M. J. G. Veltman, Nucl. Phys. B **160**, 151 (1979).
- [24] F. V. Tkachov, Phys. Lett. B **100** (1981) 65.
- [25] K. G. Chetyrkin and F. V. Tkachov, Nucl. Phys. B **192** (1981) 159.
- [26] T. Gehrmann and E. Remiddi, Nucl. Phys. B **580**, 485 (2000) [arXiv:hep-ph/9912329].
- [27] V. A. Smirnov, Berlin, Germany: Springer (2006) 283 p
- [28] R. Harlander, P. Kant, L. Mihaila and M. Steinhauser, JHEP **0609** (2006) 053 [hep-ph/0607240].
- [29] R. V. Harlander, D. R. T. Jones, P. Kant, L. Mihaila and M. Steinhauser, JHEP **0612** (2006) 024 [hep-ph/0610206].
- [30] S. S. AbdusSalam, B. C. Allanach, H. K. Dreiner, J. Ellis, U. Ellwanger, J. Gunion, S. Heinemeyer and M. Kraemer *et al.*, arXiv:1109.3859 [hep-ph].
- [31] A. I. Davydychev and M. Y. Kalmykov, Nucl. Phys. B **699** (2004) 3 [arXiv:hep-th/0303162].
- [32] A. I. Davydychev and M. Y. Kalmykov, Nucl. Phys. B **605** (2001) 266 [arXiv:hep-th/0012189].
- [33] H. Czyz, A. Grzelinska and R. Zabawa, Phys. Lett. B **538** (2002) 52 [arXiv:hep-ph/0204039].
- [34] A. V. Kotikov, Phys. Lett. B **254**, 158 (1991).
- [35] D. J. Broadhurst, J. Fleischer and O. V. Tarasov, Z. Phys. C **60** (1993) 287 [arXiv:hep-ph/9304303].
- [36] J. Fleischer, A. V. Kotikov and O. L. Veretin, Nucl. Phys. B **547**, 343 (1999) [arXiv:hep-ph/9808242].
- [37] A. I. Davydychev and J. B. Tausk, Nucl. Phys. B **397** (1993) 123.
- [38] F. A. Berends, A. I. Davydychev, V. A. Smirnov and J. B. Tausk, Nucl. Phys. B **439** (1995) 536 [arXiv:hep-ph/9410232].